A histone deacetylase confers plant tolerance to heat stress by controlling protein lysine deacetylation and stress granule formation in rice

Zhengting Chen, Qiutao Xu, Jing Wang, Hebo Zhao, Yaping Yue, Biao Liu, Lizhong Xiong, Yu Zhao, Dao-Xiu Zhou

Cell Reports

Article

A histone deacetylase confers plant tolerance to heat stress by controlling protein lysine deacetylation and stress granule formation in rice

Graphical abstract

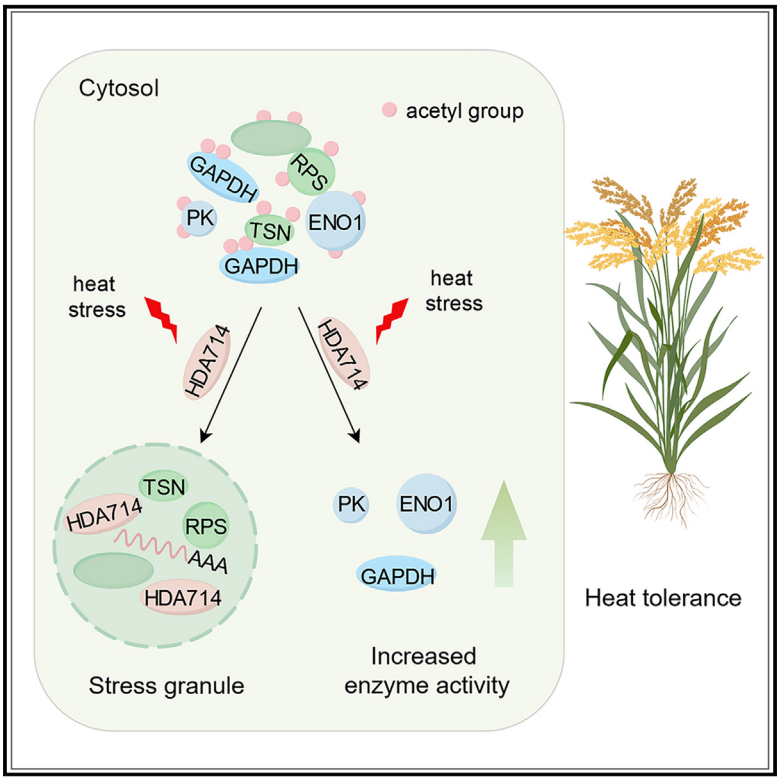

Highlights

- HDA714 responds and enhances rice tolerance to heat stress
- Heat stress leads to decreased cellular protein acetylation levels, dependent on HDA714
- HDA714 is involved in stress granule formation and stimulates glycolysis by deacetylation

Authors

Zhengting Chen, Qiutao Xu, Jing Wang, ..., Lizhong Xiong, Yu Zhao, Dao-Xiu Zhou

Correspondence

zhaoyu@mail.hzau.edu.cn (Y.Z.), dao-xiu.zhou@universite-paris-saclay.fr (D.-X.Z.)

In brief

Chen et al. demonstrate that the cytoplasmic histone deacetylase HDA714 enhances rice plant tolerance to heat stress by reducing cell protein acetylation levels. HDA714-mediated protein deacetylation promotes heat-induced stress granule formation and stimulates glycolysis for stress tolerance.

Chen et al., 2024, Cell Reports *43*, 114642
September 24, 2024
https://doi.org/10.1016/j.celrep.2024.114642

CellPress

Cell Reports

CellPress
OPEN ACCESS

Article

A histone deacetylase confers plant tolerance to heat stress by controlling protein lysine deacetylation and stress granule formation in rice

Zhengting Chen,[1,4] Qiutao Xu,[1,2,4] Jing Wang,[1] Hebo Zhao,[1] Yaping Yue,[1] Biao Liu,[1] Lizhong Xiong,[1] Yu Zhao,[1,*] and Dao-Xiu Zhou[1,3,5,*]

[1]National Key Laboratory of Crop Genetic Improvement, Hubei Hongshan Laboratory, Huazhong Agricultural University, Wuhan 430070, China

[2]State Key Laboratory for Conservation and Utilization of Subtropical Agro-bioresources, College of Agriculture, Guangxi University, Nanning 530004, China

[3]Institute of Plant Science Paris-Saclay (IPS2), CNRS, INRA, University Paris-Saclay, 91405 Orsay, France

[4]These authors contributed equally

[5]Lead contact

*Correspondence: zhaoyu@mail.hzau.edu.cn (Y.Z.), dao-xiu.zhou@universite-paris-saclay.fr (D.-X.Z.)

https://doi.org/10.1016/j.celrep.2024.114642

SUMMARY

Understanding molecular mechanisms of plant cellular response to heat stress will help to improve crop tolerance and yield in the global warming era. Here, we show that deacetylation of non-histone proteins mediated by cytoplasmic histone deacetylase HDA714 is required for plant tolerance to heat stress in rice. Heat stress reduces overall protein lysine acetylation, which depends on HDA714. Being induced by heat stress, HDA714 loss of function reduces, but its overexpression enhances rice tolerance to heat stress. Under heat stress, HDA714-mediated deacetylation of metabolic enzymes stimulates glycolysis. In addition, HDA714 protein is found within heat-induced stress granules (SGs), and many SG proteins are acetylated under normal temperature. HDA714 interacts with and deacetylates several SG proteins. HDA714 loss of function increases SG protein acetylation levels and impairs SG formation. Collectively, these results indicate that HDA714 responds to heat stress to deacetylate cellular proteins, control metabolic activities, stimulate SG formation, and confer heat tolerance in rice.

INTRODUCTION

Plants are highly sensitive to temperature variations, which have significant impacts on plant growth and development.[1] In particular, high temperatures can accelerate plant flowering and aging and reduce seed production and crop yield. It is estimated that each degree Celsius increase in global average temperature can reduce crop yield by 3%–8%.[2] Plants have developed a range of regulatory mechanisms to cope with heat stress, including protein folding, reactive oxygen species homeostasis, epigenetic modifications, and gene transcription.[1] Epigenetic modifications, such as histone acetylation, play a crucial role in plant adaptation to adverse environmental conditions. Histone acetyltransferase and histone deacetylases (HDACs) are largely involved in the epigenetic regulation of stress-responsive gene expression.[3–6] Several HDACs have been shown to control plant tolerance to high temperature or heat stress by epigenetic regulation of gene expression. For instance, Arabidopsis HDA15 interacts with the transcription factor long hypocotyl in far red1 (HFR1) to synergistically inhibit plant response to high temperatures, whereas HDA9 and HDA19 play a positive role in the response.[7] In addition, HD2B and HD2C were shown to interact with ARGONAUTE4 to promote DNA methylation and maintain heterochromatin stability under heat stress.[8] Besides histones, lysine acetylation is detected in many proteins of diverse cellular pathways. Apart from regulating histone acetylation, HDACs also deacetylate non-histone proteins to control plant response to stress. For example, HDA9 deacetylates and inhibits WKRY53, a master transcriptional regulator of stress-responsive genes in Arabidopsis.[9] SRT1, a sirtuin-type deacetylase, reduces the lysine acetylation of the glycolytic enzyme glyceraldehyde-3-phosphatedehydrogenase (GAPDH), affecting its nuclear accumulation that is enhanced by oxidative stress.[10] HDA714, a member of the rice RPD3 family, localizes in the cytoplasm and was reported as a major non-histone deacetylase in rice.[11] Protein acetylation analysis revealed that in addition to metabolic enzymes and ribosomal proteins, HDA714 deacetylates many proteins involved in stress response,[11] suggesting that protein acetylation status may be involved in plant stress response. However, the precise molecular mechanism and functional implication of non-histone protein lysine acetylation in plant stress response have yet to be fully elucidated.

Another aspect of plant response to stress, which has gained increasing attention in recent years, is stress granule (SG)

formation.[12–14] SGs are membrane-less aggregates of mRNA, proteins, and other molecules that are assembled instantaneously by liquid-liquid phase separation (LLPS) when cells are stressed.[15] SGs contain translationally stalled mRNA, translation initiation factors, RNA-binding proteins (RBPs), heat-shock proteins (HSPs), and other stress-related proteins.[16–18] SGs are disassembled during recovery from stress, allowing restoration of protein activities.

In plants, SGs form in response to diverse stresses, including heat, hypoxia, high salt, darkness, and chemical stress.[19] Several RBPs have been identified as integral components of plant SGs[14,20] and undergo phase separation to promote plant survival in response to heat stress.[13,14,21] SGs play a crucial role in conferring plant resistance to stress, protecting related proteins and mRNA, and regulating translation.[14,21] Despite the growing interest in SGs, the regulation of SG dynamics in plants remains poorly understood.

Studies in yeast and mammalian cells have shown that the acetylation of SG-associated proteins can affect SG formation.[22,23] For example, in yeast, acetylation of the RBP Pab1 at lysine 131 was found to decrease SG formation under glucose-deprivation conditions.[23] In mammalian cells, the histone deacetylase HDAC6 was shown to promote SG formation by deacetylating RNA helicases DDX3X and G3BP1, allowing their entry to SGs.[24,25] There is evidence that SG formation in plants is regulated by protein post-translational modifications, such as phosphorylation and ubiquitination,[26] but the role of protein acetylation in SG regulation is not well understood.

In this work, we show that plant response to heat stress involves a deacetylation process of cellular proteins, which depends on the rice cytoplasmic histone deacetylase HDA714. The function of HDA714 to deacetylate cellular proteins is required for rice plant tolerance to heat stress. We show that HDA714 is present in heat-induced SGs and is required for SG formation likely through the deacetylation of SG proteins. The results reveal that lysine deacetylation of cellular proteins is a cellular response to heat stress involving histone deacetylase in plants.

RESULTS

HDA714 is a positive regulator of heat stress tolerance in rice

The rice cytoplasmic histone deacetylase HDA714 was shown to control ribosomal protein lysine acetylation and translational activity.[11] To study whether HDA714 was involved in plant response to stress, we tested the heat stress tolerance of independent *hda714#1* and *hda714#2* CRISPR lines (Figure S1A). Under normal growth temperature conditions (25°C), both *hda714#1* and *hda714#2* mutant seedlings showed no visible phenotype (Figure 1A), consistent with previous observations.[11] However, the mutants exhibited lower survival rates than the wild type (WT) after recovery from heat stress (42°C) over a 5-day period (Figure 1A). Conversely, *HDA714* overexpression (OE) plants showed higher survival rates than the WT (Figure 1B), indicating that *HDA714* had a function to confer heat tolerance in rice. In contrast, *hda714#1* and *hda714#2* had no clear effect under other abiotic stresses, including cold (4°C), salt (180 mM NaCl), and drought (20% PEG6000) (Figures S1B–S1D). This would suggest that HDA714 mainly functions to confer heat stress tolerance. We further evaluated the role of HDA714 in heat stress tolerance at the reproductive stage. Under normal rice growth conditions (30°C/13 h light, 25°C/11 h dark), WT, *hda714*, and *HDA714* OE plants showed similar seed-setting rates (Figures S2A and S2B). However, under higher daytime temperatures (37°C/13 h light, 25°C/11 h dark), the seed-setting rates of *hda714* plants were lower, while those of *HDA714* OE plants were higher than the WT plants (Figures S2A and S2B). The 1,000-grain weight and -grain width of WT and *HDA714* OE plants were similar but higher than that of *hda714* plants under both normal and higher temperatures (Figures S2C and S2D). These results indicate that HDA714 has a function to confer heat tolerance at both vegetative and reproductive stages of rice plants.

HDA714 reduced the overall protein acetylation under heat stress

qRT-PCR analysis showed that the HDA714 transcript level was gradually increased during the first 60 h at 42°C (Figure 1C). The HDA714 protein was continuously accumulated during 7 days at 42°C (Figure 1D). Previous results showed that HDA714 deacetylates cytoplasmic proteins.[11] To test whether heat stress affected overall protein acetylation, using a commercial anti-Lys-acetylation antibody that detects only acetylated proteins, we analyzed cellular protein acetylation levels by immunoblotting total proteins extracted from WT and mutant seedlings treated at 25°C or 42°C for 3 days. In WT rice plants, the overall protein acetylation was clearly decreased at 42°C (Figure 2), suggesting that heat stress induced a process of deacetylation of cellular proteins. By contrast, the *hda714* mutations impaired the heat-induced protein deacetylation (Figure 2). For comparison, the mutants of two other reported cytoplasmic HDACs, which regulate some non-histone proteins in rice,[11] had no effect on the heat-induced protein deacetylation (Figures S3A and S3B). To verify the immunoblotting results, we performed quantitative acetylproteomic analysis of WT plants under normal and heat stress (42°C) conditions. Data obtained from the two biological replicates were highly correlated (Figure S4A). The acetylation levels were calibrated relative to protein abundance to prevent bias. The acetylome results showed that heat stress clearly reduced the protein acetylation levels (Figures S4B and S4C; Data S1), in line with the immunoblot results (Figure 2). The proteins with decreased Kac levels under heat stress were enriched in amide biosynthetic process, translation, gene expression, glycolytic process, and response to heat (Figure S4D). More than 50% of the proteins that show hyper (increased)-acetylation in *hda714* mutant were found to be hypoacetylated (reduced) in WT plants under heat stress (Figure S4E). These results indicate that heat stress decreases overall protein acetylation in rice plants and that HDA714 plays an important role in the process. These observations, together with the mutant phenotype in Figure 1, suggest that HDA714 is involved in heat stress tolerance, likely through deacetylation of cellular proteins.

CellPress
OPEN ACCESS

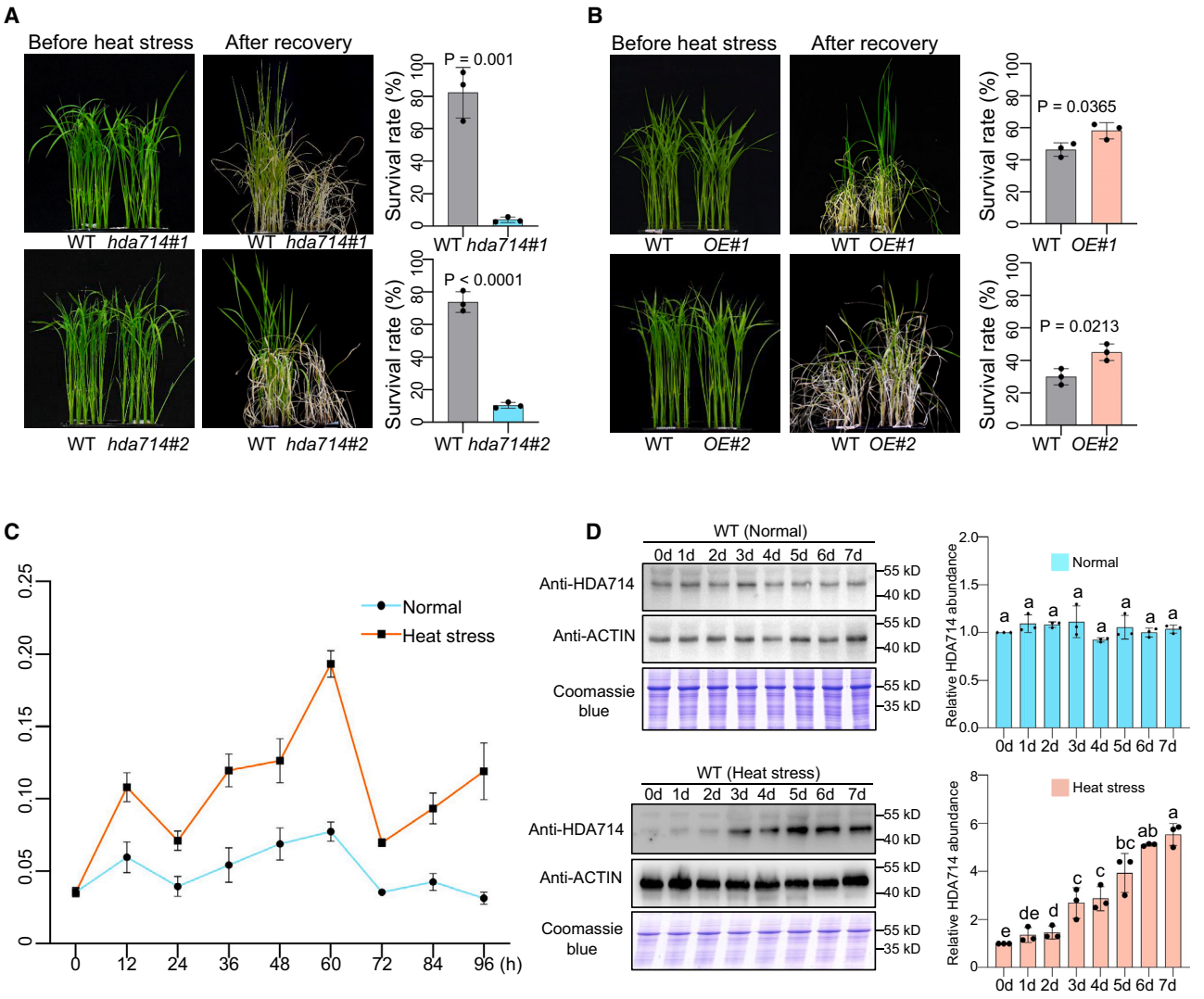

Figure 1. HDA714 is required for heat stress tolerance in rice

(A) Phenotypes of WT and *hda714* seedlings before (left) and after (right) recovery from heat stress (42°C).

(B) Phenotypes of WT and *HDA714* OE seedlings before (left) and after (right) recovery from heat stress (42°C). Seedlings were stressed at 42°C for 5 (A) or 7 (B) days, then moved to normal temperature (25°C) to recover for 7 days. The survival rates of the plants after recovery were surveyed in three biological replicates (n = 40 plants for each replicate). Significant difference was calculated by the two-tailed, paired Student t test.

(C) qRT-PCR analysis of *HDA714* transcription levels in WT under normal (25°C) and heat stress conditions (42°C) at different time points. Bars are means ± SDs from three biological replicates.

(D) HDA714 protein levels in WT seedlings under normal (25°C, top) or heat stress (42°C, bottom) conditions at different time points detected by immunoblotting with anti-HDA714. Statistical analysis for immunoblot is shown on the right. Anti-actin antibody and Coomassie blue staining were used as the loading controls of the immunoblots. Immunoblotting bands were quantified using ImageJ, and the relative signals indicated below each band were normalized with 0 day set as 1. For all statistics, the means ± SDs of three independent biological replicates are shown. The significance was calculated using one-way ANOVA with Tukey's multiple comparison tests. Different letters on top of the bars indicate a significant difference ($p < 0.05$).

HDA714 promotes the activity of glycolysis enzymes under heat stress

It has been shown that glycolysis plays a pivotal role in mediating a plant response to abiotic stresses[27–30] and that acetylation modulates the activity of glycolytic enzymes.[3,10] Examination of the rice acetylomes found that several glycolytic enzymes showed reduced acetylation levels under heat stress (Figure S4C), and their acetylation levels were found to be increased in *hda714* relative to WT plants grown in normal conditions[11] (Figures 3A and 3B). To determine whether acetylation levels in these enzymes affected their activities, we extracted proteins from the aerial parts of *hda714* and WT seedlings under normal and heat stress conditions, and tested the enzymatic activities of GAPDH, enolase (ENO), and pyruvate kinase (PK). At normal temperatures, the tested enzymes exhibited a lower activity in the mutants than the WT (Figure 3C). Under heat stress

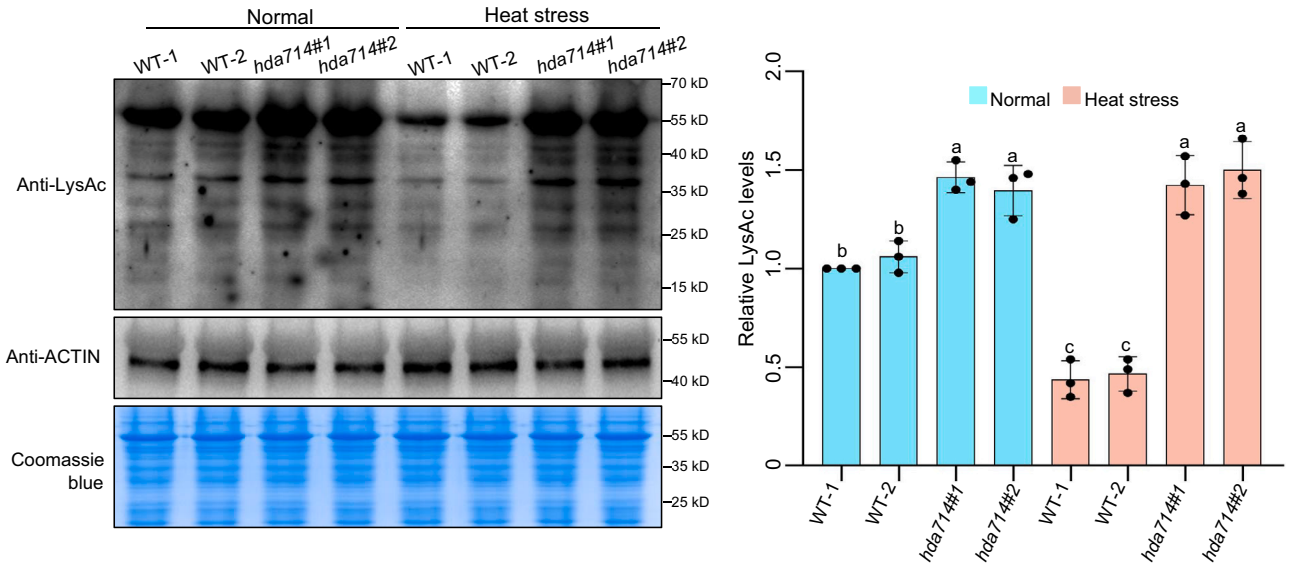

Figure 2. Heat stress reduces the overall protein acetylation levels, and the reduction requires HDA714

Overall protein lysine acetylation levels in 14-day-old WT plants (with two repetitions −1 and −2) and two independent CRISPR mutant lines (*hda714#1* and *hda714#2*) grown at 25°C or 42°C for 3 days, detected by immunoblotting with a commercial antibody (anti-LysAc) that detects only acetylated proteins. Statistical analysis for immunoblot is shown at right. Anti-actin antibody and Coomassie blue staining were used as loading controls. The immunoblotting bands were quantified using ImageJ, and the relative signals, indicated below the bands, were normalized, with WT-1 at 25°C, set as 1.

For all statistics, the means ± SDs of three independent biological replicates are shown. The significance was calculated using one-way ANOVA with Tukey's multiple comparison tests. Different letters on top of the bars indicate a significant difference ($p < 0.05$).

(42°C for 6 h), the enzymatic activities increased in the WT but remained unchanged in *hda714* plants (Figure 3C). The protein levels of GAPDH and ENO1, as detected by immunoblotting with their antibodies, were about the same in WT and *hda714* seedlings under both normal and heat stress conditions (Figure 3D). However, heat stress decreased the acetylation levels of the enzymes in the WT, as detected by anti-Lys-Ac antibody, but not in *hda714* plants (Figure 3E), confirming the acetylome data. Because of lack of PK1 antibody, we used a *pk1* mutant line complemented by HA (hemagglutinin)-PK1 (see method details). The acetylation level of HA-PK1 in the complementation plants was decreased by heat (Figure S5A), while the protein level remained similar under normal and heat stress conditions (Figure S5B). To further confirm the deacetylation of glycolytic enzymes by HDA714, we produced and purified glutathione S-transferase (GST)-tagged ENO1 and GAPDH1 proteins in *Escherichia coli* and incubated with or without HDA714 (tagged by maltose-binding protein [MBP]) for *in vitro* deacetylation assays. In the absence of HDA714, the tagged ENO1 and GAPDH1 showed high levels of lysine acetylation, indicating that the proteins were acetylated in *E. coli* cells (Figure S6). The presence of HDA714 largely reduced their acetylation levels (Figure S6). Together, these results suggest that HDA714 is involved in heat-induced deacetylation of glycolytic enzymes, which stimulates glycolysis.

HDA714 localizes in heat-induced SGs

To further investigate the mechanism underlying the HDA714-mediated heat tolerance, we next examined the subcellular localization of HDA714-GFP fusion proteins in infiltrated tobacco leaf cells. Under normal conditions, HDA714-GFP signals were evenly distributed throughout the cytosol (Figure S7A). However, after 30 min at 42°C, small granule-like structures spontaneously formed, which gradually increased in size to become larger puncta after 1 h of treatment (Figure S7A). The HDA714-containing granules displayed high degrees of co-localization (Pearson correlation coefficient [PCC] >0.82) with the SG marker proteins RBP47B[17] and TSN[12] (Figures 4A and 4B), suggesting that HDA714 localized in heat-induced SGs. To rule out the possibility that puncta formation was triggered by GFP/RFP dimerization, we examined the subcellular localization of another cytosolic histone deacetylase, HDA706.[11] No granule-like structure was formed in HDA706-GFP/RFP-infiltrated cells under normal and stressed conditions (Figure S7B). Furthermore, immunostaining of rice root cells with anti-HDA714 also revealed the formation of granule-like structures under heat stress (Figures 4C and S7C), and the addition of cycloheximide (CHX), a stable polymeric translation inhibitor that inhibits SG formation, abolished HDA714 particle formation (Figure 4C). To further confirm the observations, we isolated SG fractions from rice seedlings under both normal and heat stress conditions using a previously described procedure (Figure 5A)[31] and analyzed the isolated SG fractions by immuno-inflorescence and immunoblotting with the HDA714 antibody. The analyses detected high enrichments of the HDA714 protein in the heat-induced SG fractions relative to those from the control condition (Figures 5B and 5C).

Identification of heat-induced SG proteome in rice cells

To characterize heat-induced HDA714-containing SGs, using anti-HDA714 antibody we affinity purified the SG fractions

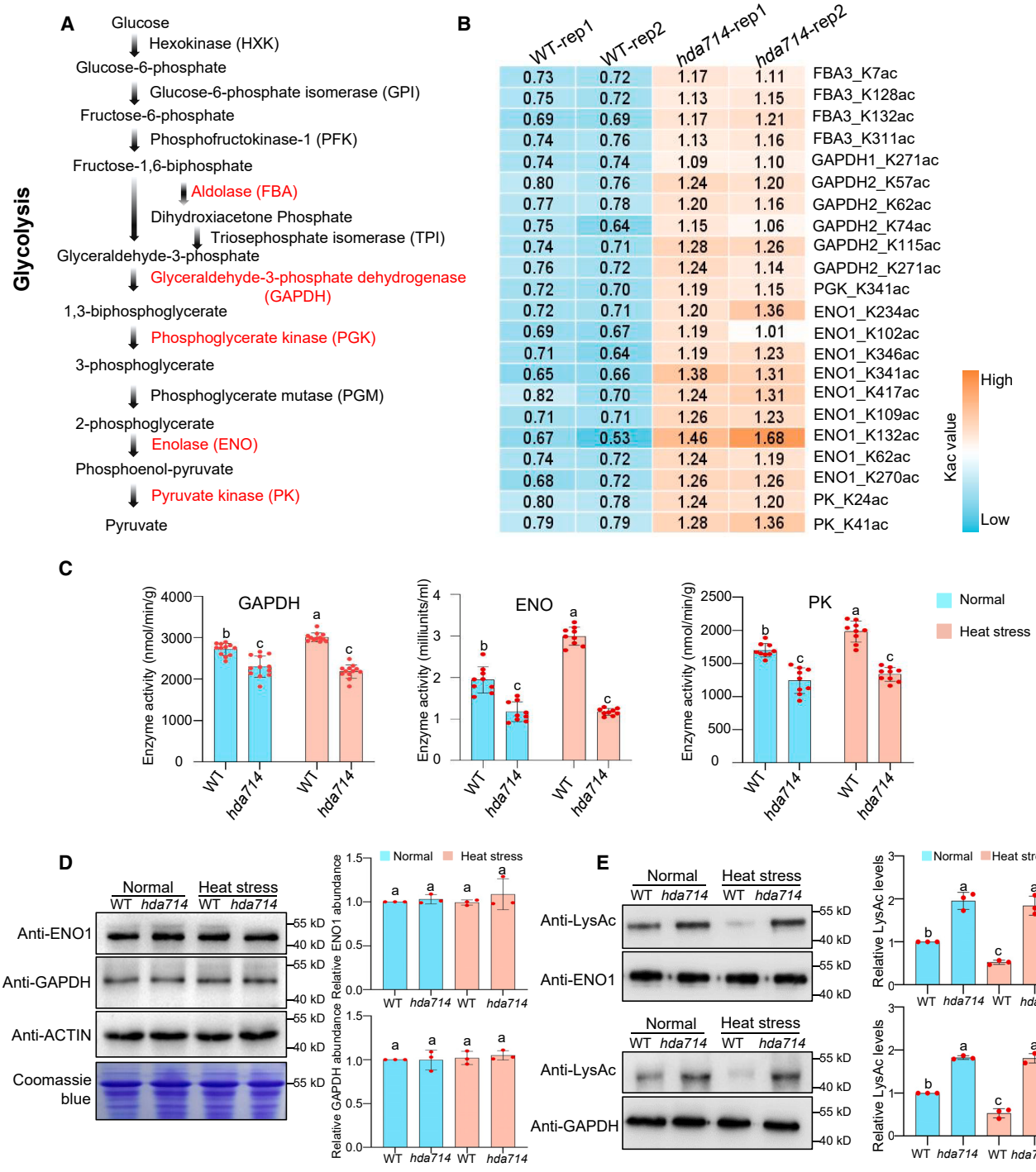

Figure 3. HDA714 promotes glycolysis by deacetylation under heat stress

(A) Overview of the glycolytic pathway. Enzymes with increased acetylation in *hda714* are labeled in red.

(B) Heatmaps of acetylation levels at individual lysine residues of glycolytic enzymes in *hda714* and WT.

(C) Enzyme activity assays of GAPDH, ENO, and PK in *hda714* and WT plants under normal (25°C) and heat stress (42°C for 6 h) conditions.

(D) ENO1 and GAPDH protein levels in WT and *hda714* plants under normal and heat stress conditions, detected by immunoblotting with anti-ENO1 and anti-GAPDH antibodies, respectively. Statistical analysis for immunoblot is shown at right. Anti-actin antibody and Coomassie blue staining were used as loading controls. Immunoblotting bands were quantified using ImageJ and the relative signals for statistics analysis were normalized with WT under normal conditions (set as 1).

(legend continued on next page)

isolated from the control and stress-treated seedlings and analyzed the immuno-purified SGs by mass spectrometry (MS)-based proteomics (Figures 5A and 5D). In the heat-stress group, 510 proteins (with unique peptides >2 as criterion) were identified in all three biological replicates, compared with 33 in the control groups (Figure S8A). After eliminating those overlapping with the proteins in the control and the proteins annotated as plastid and mitochondrial proteins, 223 proteins (Figure S8B; Data S2) were identified as present in heat-induced SGs in rice seedlings. HDA714 was among the 223 heat-induced SG proteins (Data S2).

Among the 223 candidate SG proteins, 30 and 24 were in common, respectively, with previously published human and Arabidopsis SGs,[16,17] with 10 commonly found in the 3 organisms (Figure S8C; Data S3). The 10 SG proteins included 3 well-characterized SG marker proteins: 2 homologous to poly(A)-binding protein (PABP3),[12,17] one to Tudor protein with multiple SNc domains (TSN),[12,17] and 4 HSP (chaperones). According to published rice acetyl-proteomic data,[11,32] the 10 proteins are acetylated in normal growth conditions. Recently, salicyclic acid (SA)-induced SG proteins were reported in Arabidopsis,[33] with which 153 of the 223 rice SG proteins overlapped (Figure S8D).

Functional classification and Gene Ontology pathway analysis of the 223 rice candidate SG proteins revealed an enrichment of translation, gene expression, chaperone, and RNA metabolism proteins (Figures S9A and S9B). According to present and published rice protein acetylomes,[11] 199 of the 223 proteins are acetylated (Figure S9C). Among the 199 acetylated SG proteins, 155 showed decreased acetylation under heat stress in WT (Figure S9D), 97 of which displayed increased acetylation in *hda714* in normal conditions[11] (Figure S9D) A domain analysis of the candidate SG proteins revealed an enrichment of prion and ATPase motifs (Data S4), which were recognized as essential elements for the assembly or dynamics of SGs in previous studies.[16,17,22]

To validate the rice SG proteome, we made GFP fusions with eight candidate proteins, including TSN, PABPC1, and PABPC3, as well as ribosomal proteins RPS3 and RPS6, elongation factor EIF, DEAD-box ATP-dependent RNA helicase DEAD, and PK3, and analyzed their presence in heat-induced SGs in tobacco leaf cells (Figures S10A–S10H). The analysis showed that all of the fusion proteins exhibited aggregation into cytosolic foci under heat stress, overlapping with the SG marker protein RBP47B-RFP (Figures S10A–S10H). The results confirmed that they were *bona fide* SG proteins in rice plants.

HDA714 interacts with several SG proteins in rice cells and is required for RPS6 entry into heat-induced SGs

RPS6 is a component of the small subunit of ribosomes and has been reported as an SG protein in animal and plant cells.[18,33] It was previously shown that HDA714 interacts with and deacetylates RPS6.[11] Analysis of RPS6 subcellular localization in HDA714-FLAG plants by anti-RPS6 immunofluorescence indicated that RPS6 was diffused throughout the cytoplasm in rice root cells at a normal temperature (25°C), but was condensed in cytoplasmic foci and co-localized with the HDA714-FLAG protein under heat stress (Figure 6A). The results suggested that both proteins were recruited to the same SGs in rice cells.

To test whether HDA714 was required for RPS6 entry into SGs, we examined RPS6 subcellular localization in WT and *hda714* mutant plants (Figure 6B). The results showed that heat stress-induced RPS6-containing SGs were largely reduced in *hda714* cells compared to the WT (Figures 6B and 6C). To examine whether HDA714 function in RPS6 SGs was related to its deacetylase activity, we treated rice plants with trichostatin A (TSA), a specific HDAC inhibitor, and examined the formation of heat-induced RPS6 particles. The results revealed a clear reduction of RPS6-containing SGs by TSA (Figures S11A and S11B), suggesting that the function of HDA714 in heat-induced RPS6 SG formation depends on its deacetylase activity.

In addition, HDA714 could interact with other SG proteins TSN and PK3 *in vivo* and *in vitro* (Figures S12A–S12D). The interactions could be detected at normal temperatures and also under heat stress within SGs (Figure S12A). To confirm the function of HDA714 in heat-induced SG formation, we used TSN, an SG core marker protein,[12] to make GFP fusion and transfected WT and *hda714* cells. Heat stress induced the formation of a much lower number of SGs in the mutant than WT cells (Figure S13A). The results support the hypothesis that the *HDA714* has a function in heated-induced SG formation.

HDA714-mediated deacetylation is required for heat-induced SG formation in rice cells

From the published acetyl-proteomic data,[11] the acetylation levels of 107 rice SG proteins were augmented in *hda714* plants (Figure S9D). To test whether HDA714 was required for the deacetylation of SG proteins under heat stress, SG fractions were isolated from heat-stressed WT, *hda714*, and *HDA714* overexpression plants, as described in Figure 5. The SG-enriched fractions were analyzed by immunoblotting using the anti-LysAc antibody that detects only acetylated proteins. The results showed that the overall protein acetylation levels of heat-induced SGs were much higher in the *hda714* mutant, but lower in OE, than WT plants (Figure 7A). To test the acetylation levels of individual SG proteins, we immuno-purified RPS6 (with anti-RPS6) from the isolated SG fractions and analyzed its acetylation level by immunoblotting using anti-LysAc antibody. The analysis revealed that the RPS6 acetylation level was higher in the SGs isolated from *hda714* mutant and lower from *HDA714* OE than from WT plants (Figure 7B).

To further test whether lysine acetylation of RPS6 affected its presence in SGs, we made lysine acetylation mimic (K to Q) and

(E) ENO1 and GAPDH protein acetylation levels in WT and *hda714* plants under normal and heat stress conditions. The ENO1 and GAPDH proteins were first immuno-purified from the plant protein extracts using anti-ENO1 or anti-GAPDH antibodies coated on protein-A beads, then analyzed by immunoblotting with the anti-LysAc antibody. Statistical analysis for immunoblot is shown at right. Anti-ENO1 and anti-GAPDH were used to control the loaded protein levels. Immunoblotting bands were quantified using ImageJ, and the relative signals for statistics analysis were normalized with WT under normal conditions (set as 1).
For all statistics, the means ± SDs of three independent biological replicates are shown. The significance was calculated using one-way ANOVA with Tukey's multiple comparison tests. Different letters on top of the bars indicate a significant difference ($p < 0.05$).

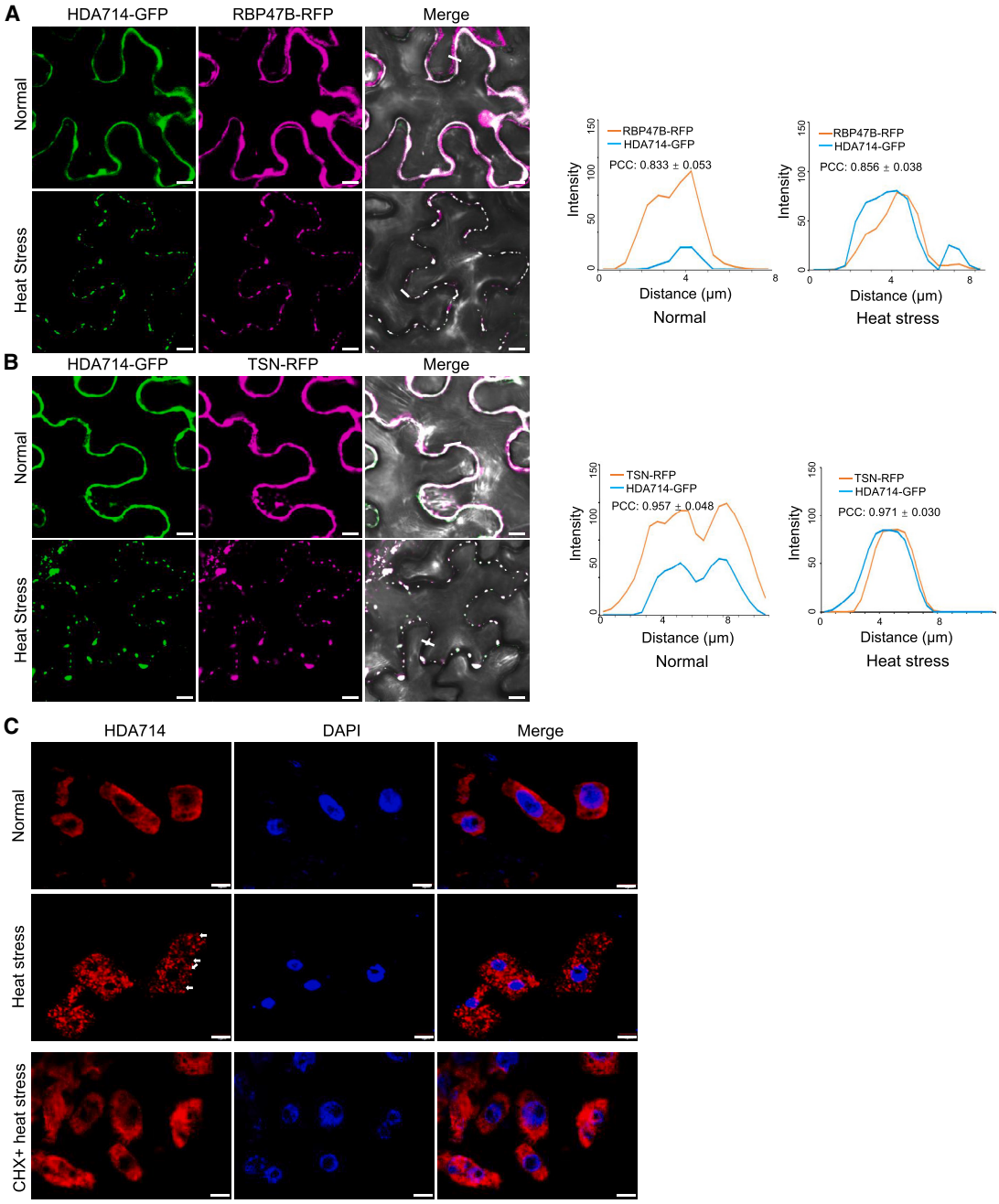

Figure 4. HAD714 localizes in heat-induced SGs

(A and B) Subcellular localization of HDA714-GFP in tobacco epidermal cells under normal (25°C) and heat stress conditions (42°C for 30 min). RFP-tagged RBP47B or TSN served as a SG marker. Scale bars, 10 μm. The HDA714 coding sequence was fused to GFP at its C terminus. The coding sequences of RBP47B and TSN were each fused to RFP at their respective C termini. All fusion constructs were placed under the control of the cauliflower mosaic virus 35S promoter. At least three tobacco plants (n = 3) were infiltrated. The related intensity profiles and PCC are shown on the left of the images. The white lines serve as typical examples representing the intensity profiles. n = 6 for PCC quantification (mean ± SD is shown).

(C) Anti-HDA714 immunostaining of rice root tip cells at 25°C and 42°C for 6 h and rice root cells pretreated with CHX (200 ng/L) for 30 min before being heat stressed at 42°C for 6 h. Arrows indicate SGs. Scale bars, 5 μm. Red (HDA714), blue (DAPI), nuclei.

For (A) and (B), to mitigate red-green color perception difficulties, red was replaced with magenta.

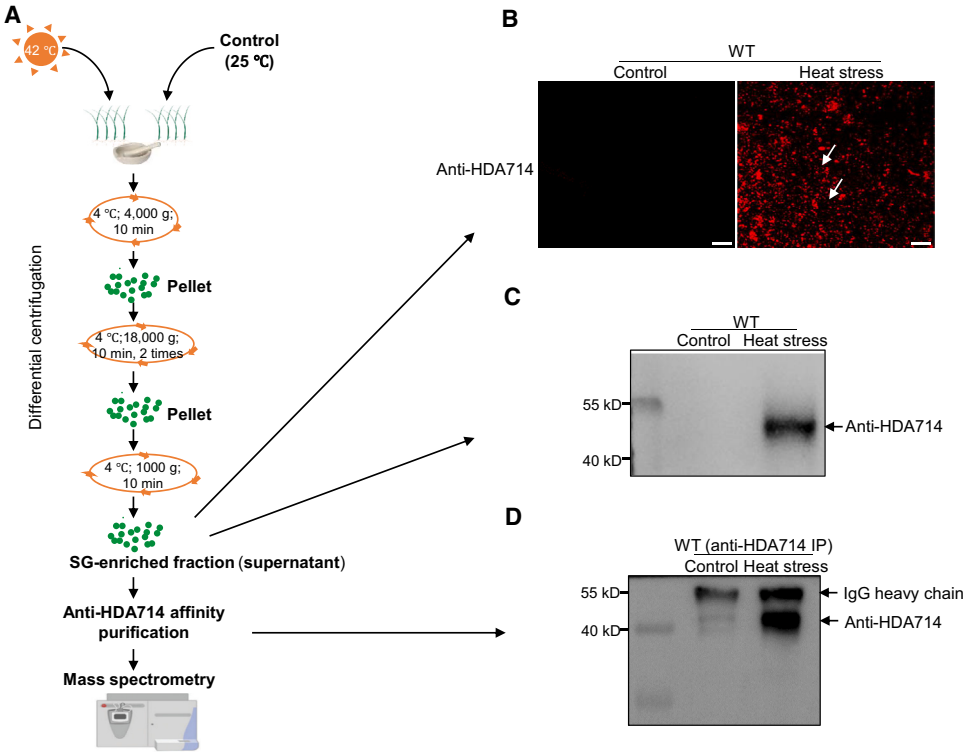

Figure 5. Identification of heat-induced SG proteins in rice

(A) Schematic representation of SG fraction isolation from rice plants and anti-HDA714 affinity purification for MS analysis. SG fractions were also extracted from heat-stressed (42°C) and control (25°C) plants using a previously described procedure.[31] Briefly, rice seedlings were grounded with liquid nitrogen and suspended in lysis buffer. After centrifugation at 4,000 × *g* for 10 min at 4°C, the pellets were washed twice in lysis buffer with centrifugation at 18,000 × *g* for 10 min at 4°C. The pellets were resuspended and centrifuged at 1,000 × *g* for 10 min at 4°C. The SG-enriched supernatants were collected for analysis in (B) and (C). For identification of HDA714-associated SG proteins, the SG-enriched fractions were affinity purified with anti-HDA714 antibody and analyzed by MS.

(B) Anti-HDA714 immunostaining of the SG-enriched fractions (arrows) isolated from heat-stressed (42°C) and control (25°C) rice plants. Scale bars, 10 μm.

(C) Immunoblotting with anti-HDA714 antibody of SG-enriched fractions from the stressed (42°C) and control (25°C) plants.

(D) Immunoblotting of anti-HDA714 immuno-precipitates from SG fraction isolated heat-stressed (42°C) and control (25°C) plants. The band at 55 kDa corresponds to the immunoglobulin G heavy chain.

resistant (K to R) point mutations in RPS6. The RPS6 lysine residues (K2, K14, K15, K23, and K157) that showed increased acetylation in *hda714* mutant,[11] were simultaneously mutated to Q or R. The RPS6 WT and the K to Q or R mutant proteins were fused with GFP and co-expressed with the SG marker RBP47B in tobacco leaf cells (Figure 7C). Under normal conditions, the WT and mutant versions of RPS6-GFP fusion were evenly distributed in tobacco cells (Figure 7C). Under heat stress, the WT and the mutations of RPS6-GFP were found to co-localize with the SG marker RBP47B-RFP (Figure 7C). However, with the lysine-acetylation resistant (K to R) mutants, a high number of SGs was observed under heat stress, while a lower number of SGs were produced with the acetyl-lysine (K to Q) mimic mutants when compared with WT RPS6 (Figure 7C, right), suggesting that lysine deacetylation stimulated RPS6 entering into SGs.

To further assess the impact of protein deacetylation on heat-induced SG formation, we made acetyl-lysine mimic (K to Q) and acetylation-resistant (K to R) mutations in the SG marker protein TSN at lysine residue 76 (K76), which exhibited an increased acetylation in the *hda714* mutant.[11] The WT and the K to Q or R mutants of the TSN protein were fused with GFP and expressed in rice cells. Under heat stress, a higher number of SGs were produced in cells transfected by the acetylation-resistant (K76 R) mutant than the WT or the acetyl-lysine mimic (K76Q) mutant (Figure S13B). To further confirm the deacetylation of TSN by HDA714, we produced GST-tagged TSN protein in *E. coli*. After purification, the tagged protein was incubated with or without HDA714-MBP in deacetylation buffer. Without HDA714, GST-TSN showed a high level of lysine acetylation (Figure S6). The presence of HDA714 reduced TSN lysine acetylation levels (Figure S6). Collectively, the results indicate that HDA714-dependent lysine deacetylation promotes heat-induced SG formation in rice cells.

DISCUSSION

Plants have evolved regulatory networks of gene expression to effectively cope with heat stress. Transcription factors are crucial components in these networks, and their activity is meticulously regulated at multiple levels to response to heat stress.[1] In the present study, we explored a previously unexplored

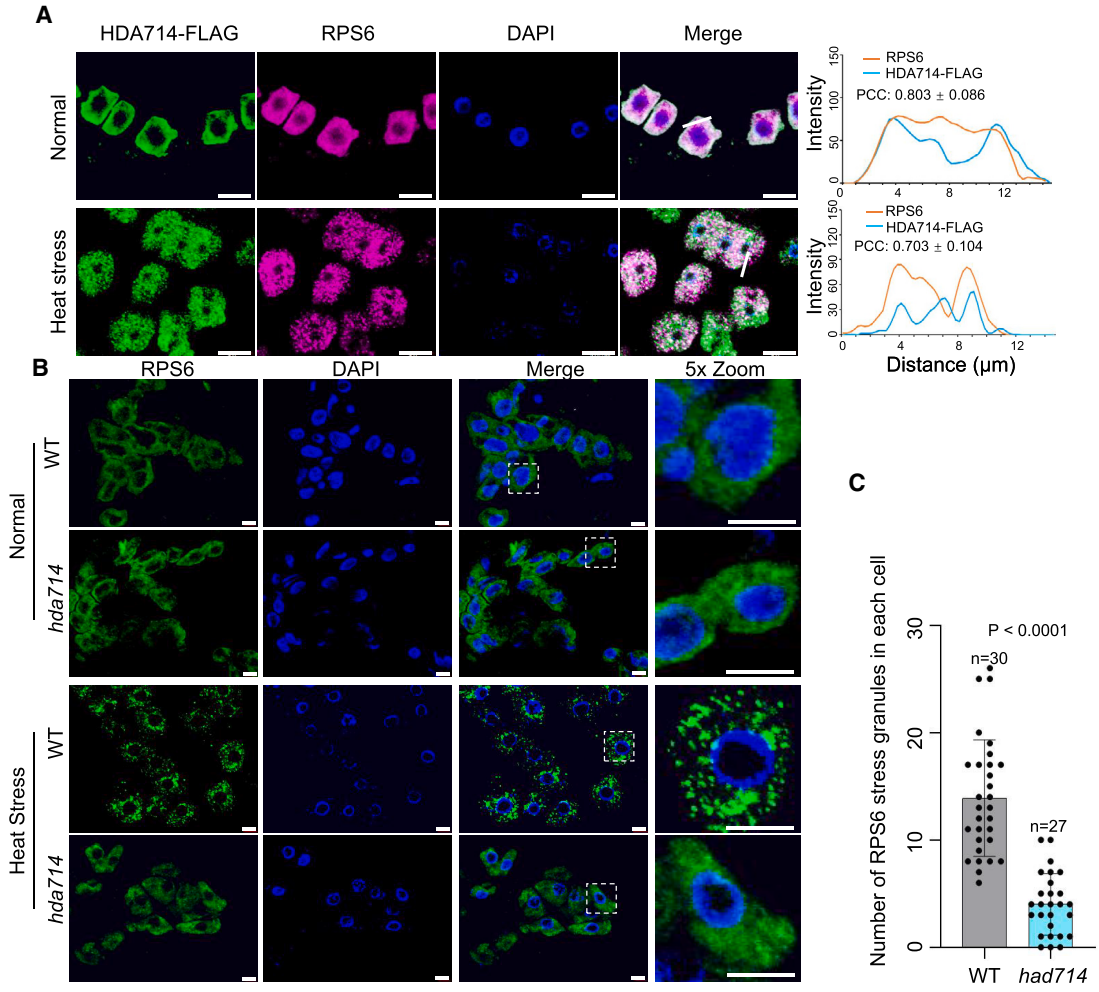

Figure 6. HDA714 is required for RPS6 entry into heat-induced SGs

(A) Subcellular localization of HDA714 and RPS6 in rice cells. HDA714-FLAG plant root tip cells were immunostained with anti-FLAG and anti-RPS6 antibodies under normal (25°C) and heat stress (42°C for 6 h) conditions. To mitigate red-green color perception difficulties, red was replaced with magenta. Scale bars, 10 μm. Nuclei are indicated by DAPI staining. GFP, HDA714-FLAG; magenta fluorescence, RPS6. The related intensity profiles and PCC are indicated at right. The white lines serve as typical examples representing the intensity profiles. $n = 6$ for PCC quantification (mean ± SD is shown). Scale bars, 10 μm.

(B) Mutation of *hda714* led to reduced RPS6-containing SG numbers in rice cells. Anti-RPS6 immunostaining was performed on the root tip cells of WT and *hda714* plants under normal (25°C) and heat stress (42°C for 6 h) conditions. Scale bars, 10 μm. Blue (DAPI): nuclei; green: RPS6.

(C) Quantification of heat-induced RPS6-containing SGs in both WT and *hda714* plants (B). SG numbers in rice root tip cells were quantified by ImageJ in individual cells. Data are presented as mean ± SD ($n \geq 27$). The significant difference between the groups was analyzed using a Student's t test.

regulatory mechanism that involves protein lysine acetylation regulated by the cytoplasmic histone deacetylase HDA714. The present work provided evidence that HDA714 is required specifically for heat tolerance, likely through the deacetylation of cytoplasmic protein in rice plants. First, the expression and protein accumulation of HDA714 are induced during heat treatment. Its loss of function impairs rice plant tolerance to heat stress, while its OE increases the tolerance. Second, heat stress leads to decreases in the overall cellular protein acetylation levels, which is at least partially dependent on HDA714. Third, HDA714 locates in heat-induced SG and is required for the SG formation. Finally, HDA714 interacts with and is required for the deacetylation of some SG proteins. However, whether HDA714 contributes to the functional recovery of SG protein after the release of heat stress deserves further investigation. These findings reveal a novel function for histone deacetylases in plants, underscoring the complexity of the regulatory networks that are involved in plant response to heat stress.

Lysine deacetylation of cellular proteins is a cellular response to heat stress in plants

Recent results have shown that besides histones, many cellular proteins, especially metabolic enzymes and translational proteins, are acetylated.[10,11,29,34] In this work, we showed that heat stress sensibly reduces the overall acetylation level of cellular proteins, which stimulates glycolytic enzymatic activities. This indicates that protein acetylation dynamics is a cellular response to heat stress. The observation that the *hda714*

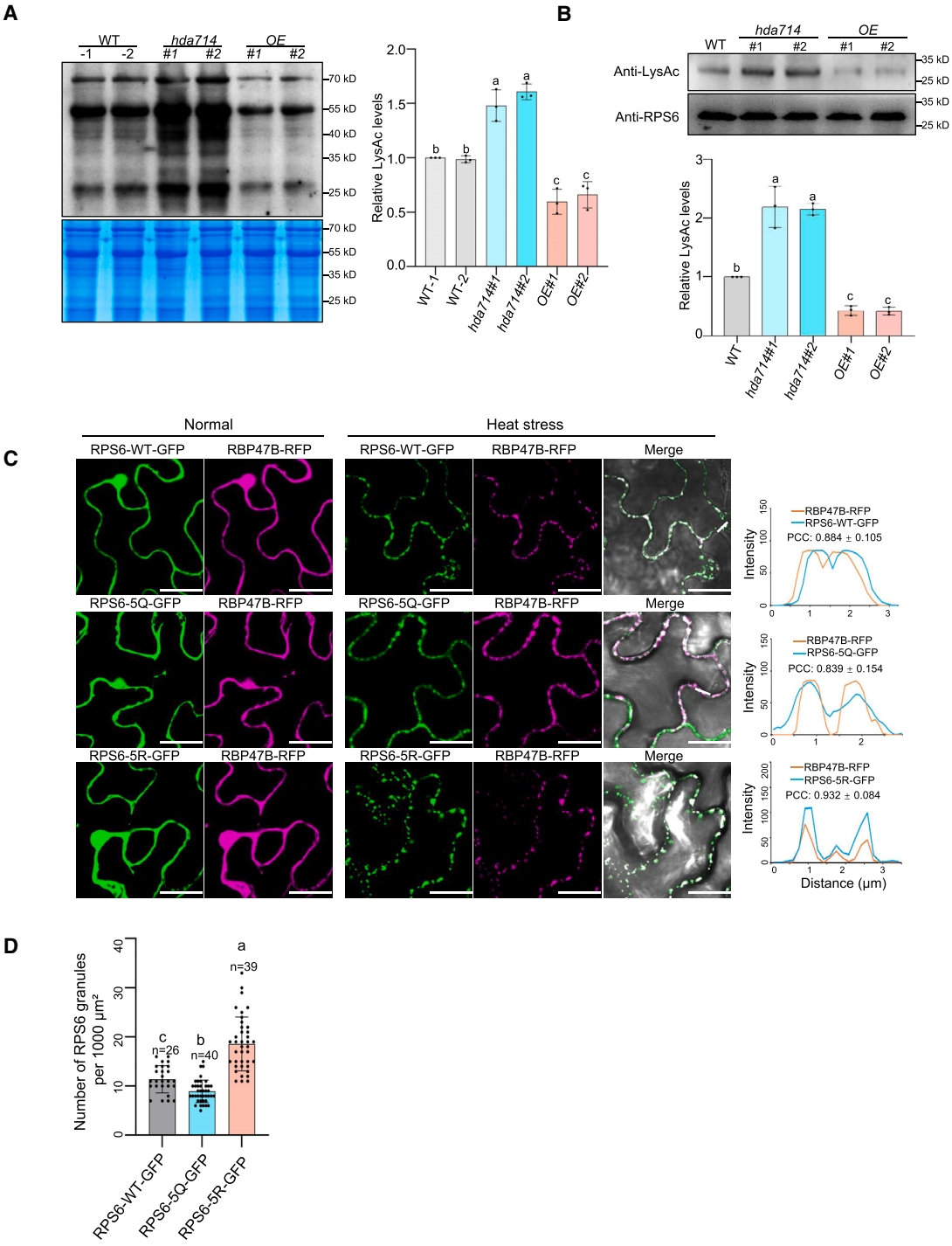

Figure 7. HDA714-mediated deacetylation of SG proteins is required for heat-induced SG formation

(A) Analysis of protein acetylation levels of SG fractions isolated from heat-treated *hda714*, *HDA714* OE in comparison with WT plants by immunoblotting using anti-LysAc antibody, which detects only acetylated proteins. Coomassie blue staining was used as loading controls. Statistical analysis for immunoblot is shown at right.

(B) Analysis of RPS6 acetylation levels in SG fractions isolated from WT, *hda714*, and *HDA714* OE plants under heat stress (42°C). Statistical analysis for immunoblot is shown at right. The SG fractions were immuno-purified with anti-RPS6 antibody-coated protein-A beads. The purifications were tested by immunoblotting with anti-LysAc to detect RPS6 acetylation and with anti-RPS6 to test RPS6 protein levels in the different samples. The immunoblotting bands were quantified using ImageJ, and the relative signals, indicated below each band, were normalized to WT, which was set to 1.

(legend continued on next page)

mutation impairs heat-induced deacetylation of cellular proteins indicates that HDA714 is at least partly responsible for the heat stress-induced protein deacetylation process. Although the function of protein lysine acetylation is unclear, previous studies indicated that lysine acetylation may promote protein poly-ubiquitination and degradation.[11,35,36] In addition, lysine acetylation can affect metabolic enzyme activities and ribosomal protein functions.[11,37] The heat stress-induced lysine deacetylation process may promote cellular protein stability, stimulate translation, and enhance metabolism such as glycolysis shown in this work, for plant tolerance.

The present work showing that the acetylation of many rice SG proteins is reduced by heat stress indicates that lysine acetylation plays a role in heat-induced SG dynamics. The effects of *hda714* mutations (as well as treatment with the deacetylase inhibitor TSA) on SG formation, combined with those of the acetylation-resistant or mimic point mutations within the TSN and RPS6 proteins, suggest that lysine acetylation controls SG protein entry or SG formation. SGs are spontaneously formed under stress to prevent the degradation of essential proteins required for cell survival.[38] The present data suggest that HDA714-mediated deacetylation of SG proteins may contribute not only to the SG formation but also to SG protein stability and functional recovery once the stress is relieved. This hypothesis is supported by previous results showing that HDA714 enhances ribosomal protein stability and translational activity under normal conditions.[11] Thus, heat stress-induced deacetylation of cellular proteins may control various cellular processes, including SG formation and translational activity to enhance tolerance to the stress. The present results also suggest that heat-induced SGs are more stable in rice plants. As shown in Figure 6, RPS6-containing SGs are robust after 6 h of heat treatment. This is also supported by the observation that SG formed after 6 h of heat treatment was prevented by CHX (Figure 4C). In addition, during heat treatment, few HDA714-containing granules appeared after 0.5 h, but many more granules appeared after 3 and 6 h (Figure S7C). SGs are formed rapidly and start to disassemble soon after the stress is gone. The persistence of SG in rice during 6 h of heat stress is consistent with previous observations of SG formation under prolonged stress in HeLa (at 44°C for 1 h)[25] and MEF (under arsenite stress for 3 h) cells,[39] and in mice fed Western food for 16 weeks.[40]

Possible function of HDA714 in heat-induced SG formation

SGs are inducible and reversible biomolecular condensates assembled by LLPS upon induction by a variety of endogenous and exogenous stresses.[38] LLPS is often triggered by proteins with intrinsically disordered regions (IDRs) that induce the aggregation of proteins or protein-RNA complexes. It was shown that protein lysine acetylation has a negative effect on LLPS, inhibiting SG assembly.[24] For instance, acetylation of lysine 376 in the RNA-binding domain of mammalian G3BP1, an SG marker protein, negatively affects its ability to bind RNA and interact with other SG components, leading to the disassembly of SG.[41] Additionally, acetylation of the IDRs of DDX3X, which is a component of SGs, hinders the formation of SGs.[24] Mammalian HDAC6 was shown to enter SGs and deacetylate DDX3X and G3BP1[24,41]. Plant homologs of G3BP-1 and DDX3X are shown to function in SGs.[42] DDX3X appears to be acetylated in rice (Data S5). Interestingly, as with several plant class II HDACs, HDA714 also contains IDRs.[43] It remains to be determined whether HDA714 directly participates in SG formation via IDR-mediated LLPS.

In conclusion, our results identify HDA714 as a heat-responsive cytoplasmic lysine deacetylase that may enhance plant tolerance to heat stress through several pathways. First, HDA714 may confer plant tolerance to heat stress by participating in and facilitating SG formation. Second, HDA714 may improve plant tolerance by enhancing metabolic activity such as glycolysis (Figure S14). In addition, the function of HDA714 that stabilizes ribosomal proteins and promotes protein translation, as shown previously,[43] may be also involved in improving plant tolerance to heat.

Limitations of the study

In this study, we have uncovered a protective role of HDA714 in rice under heat stress. However, it is essential to highlight certain limitations in our analysis. First, SG formation can be divided into formation and recovery stages. Whether HDA714 has a function in SG recovery is not yet clear. In addition, whether HDA714 controls the interaction between SG proteins and RNA remains to be studied. Second, there is a lack of field trial data to confirm the contribution of HDA714 to heat tolerance in rice grain production. In addition, the 6-h heat stress that we used in our experiments may affect the components of SG in rice. All in all, these questions are important for fully understanding the function of HDA714 in heat stress and its application in crop improvement.

STAR★METHODS

Detailed methods are provided in the online version of this paper and include the following:

- KEY RESOURCES TABLE
- RESOURCE AVAILABILITY

For (A) and (B) statistics, the means ± SDs of three independent biological replicates are shown. The significance was calculated using one-way ANOVA with Tukey's multiple comparison tests. Different letters on top of the bars indicate a significant difference ($p < 0.05$).

(C) Subcellular localization of RPS6 (WT and K to Q or R mutant) proteins in tobacco epidermal cells under heat stress (42°C for 30 min). The coding sequence of RPS6 or RBP47B was fused to GFP or RFP, respectively, at its C terminus and under the control of the cauliflower mosaic virus 35S promoter. RBP47B serves as an SG marker. To mitigate red-green color perception difficulties, red was replaced with magenta. Scale bars, 20 μm. At least three tobacco plants ($n = 3$) were infiltrated per test. The related intensity profiles and PCC of RBP47B-RFP and RPS6-GFP in SGs are shown at right. The white lines serve as typical examples representing the intensity profiles. $n = 6$ for PCC quantification (mean ± SD is shown).

(D) ImageJ quantification of RPS6-containing SGs per 1,000 μm^2 of leaf area transfected by WT and point mutation mutant (K to R or Q) of RPS6 under heat stress conditions. Data are presented as mean ± SD ($n \geq 27$). The significance was calculated using one-way ANOVA with Tukey's multiple comparison tests. Different letters on top of the bars indicate a significant difference ($p < 0.05$).

SUPPLEMENTAL INFORMATION

Supplemental information can be found online at https://doi.org/10.1016/j.celrep.2024.114642.

ACKNOWLEDGMENTS

We thank Qinglu Zhang and Xianghua Li for technical assistance. We thank Figdraw for creation of the graphical abstract. This work was supported by grants from the National Natural Science Foundation of China (no. 31821005), the Fundamental Research Funds for the Central Universities (2662023SKPY002, 2016RC003), the French Agence Nationale de la Recherche (ANR-19-CE12-0027-01), the starting research grant for High-Level Talents from Guangxi University (ZX01080033124005), and the Scientific Research and Development Fund of the College of Agriculture, Guangxi University (EE101761).

AUTHOR CONTRIBUTIONS

Z.C. and Q.X. performed most of the experiments and analyzed the data. J.W., H.Z., Y.Y., B.L., L.X., and Y.Z. contributed to the experimentation. D.-X.Z. supervised the project. D.-X.Z. analyzed the data and wrote the paper, with input from Z.C. and Q.X. All authors read and approved the final manuscript.

DECLARATION OF INTERESTS

The authors declare no competing interests.

Received: March 1, 2024
Revised: June 17, 2024
Accepted: July 31, 2024
Published: September 5, 2024

REFERENCES

1. Ding, Y., Shi, Y., and Yang, S. (2020). Molecular Regulation of Plant Responses to Environmental Temperatures. Mol. Plant *13*, 544–564. https://doi.org/10.1016/j.molp.2020.02.004.
2. Zhao, C., Liu, B., Piao, S., Wang, X., Lobell, D.B., Huang, Y., Huang, M., Yao, Y., Bassu, S., Ciais, P., et al. (2017). Temperature increase reduces global yields of major crops in four independent estimates. Proc. Natl. Acad. Sci. USA *114*, 9326–9331. https://doi.org/10.1073/pnas.1701762114.
3. Shen, Y., Wei, W., and Zhou, D.X. (2015). Histone Acetylation Enzymes Coordinate Metabolism and Gene Expression. Trends Plant Sci. *20*, 614–621. https://doi.org/10.1016/j.tplants.2015.07.005.
4. Hu, Y., Lu, Y., Zhao, Y., and Zhou, D.X. (2019). Histone Acetylation Dynamics Integrates Metabolic Activity to Regulate Plant Response to Stress. Front. Plant Sci. *10*, 1236. https://doi.org/10.3389/fpls.2019.01236.
5. Lu, Y., Bu, Q., Chuan, M., Cui, X., Zhao, Y., and Zhou, D.X. (2023). Metabolic regulation of the plant epigenome. Plant J. *114*, 1001–1013. https://doi.org/10.1111/tpj.16122.
6. Cui, X., Dard, A., Reichheld, J.-P., and Zhou, D.-X. (2023). Multifaceted functions of histone deacetylases in stress response. Trends Plant Sci. *28*, 1245–1256. https://doi.org/10.1016/j.tplants.2023.06.006.
7. Shen, Y., Lei, T., Cui, X., Liu, X., Zhou, S., Zheng, Y., Guérard, F., Issakidis-Bourguet, E., and Zhou, D.X. (2019). Arabidopsis histone deacetylase HDA15 directly represses plant response to elevated ambient temperature. Plant J. *100*, 991–1006. https://doi.org/10.1111/tpj.14492.
8. Yang, F., Sun, Y., Du, X., Chu, Z., Zhong, X., and Chen, X. (2023). Plant-specific histone deacetylases associate with ARGONAUTE4 to promote heterochromatin stabilization and plant heat tolerance. New Phytol. *238*, 252–269. https://doi.org/10.1111/nph.18729.
9. Zheng, Y., Ge, J., Bao, C., Chang, W., Liu, J., Shao, J., Liu, X., Su, L., Pan, L., and Zhou, D.X. (2020). Histone Deacetylase HDA9 and WRKY53 Transcription Factor Are Mutual Antagonists in Regulation of Plant Stress Response. Mol. Plant *13*, 598–611. https://doi.org/10.1016/j.molp.2019.12.011.
10. Zhang, H., Zhao, Y., and Zhou, D.X. (2017). Rice NAD+-dependent histone deacetylase OsSRT1 represses glycolysis and regulates the moonlighting function of GAPDH as a transcriptional activator of glycolytic genes. Nucleic Acids Res. *45*, 12241–12255. https://doi.org/10.1093/nar/gkx825.
11. Xu, Q., Liu, Q., Chen, Z., Yue, Y., Liu, Y., Zhao, Y., and Zhou, D.X. (2021). Histone deacetylases control lysine acetylation of ribosomal proteins in rice. Nucleic Acids Res. *49*, 4613–4628. https://doi.org/10.1093/nar/gkab244.
12. Gutierrez-Beltran, E., Elander, P.H., Dalman, K., Dayhoff, G.W., 2nd, Moschou, P.N., Uversky, V.N., Crespo, J.L., and Bozhkov, P.V. (2021). Tudor staphylococcal nuclease is a docking platform for stress granule components and is essential for SnRK1 activation in Arabidopsis. EMBO J. *40*, e105043. https://doi.org/10.15252/embj.2020105043.
13. Tian, X., Qin, Z., Zhao, Y., Wen, J., Lan, T., Zhang, L., Wang, F., Qin, D., Yu, K., Zhao, A., et al. (2022). Stress granule-associated TaMBF1c confers thermotolerance through regulating specific mRNA translation in wheat (Triticum aestivum). New Phytol. *233*, 1719–1731. https://doi.org/10.1111/nph.17865.
14. Zhu, S., Gu, J., Yao, J., Li, Y., Zhang, Z., Xia, W., Wang, Z., Gui, X., Li, L., Li, D., et al. (2022). Liquid-liquid phase separation of RBGD2/4 is required for heat stress resistance in Arabidopsis. Dev. Cell *57*, 583–597.e6. https://doi.org/10.1016/j.devcel.2022.02.005.
15. Allen, J.R., and Strader, L.C. (2022). Beating the heat: Phase separation in plant stress granules. Dev. Cell *57*, 563–565. https://doi.org/10.1016/j.devcel.2022.02.012.
16. Jain, S., Wheeler, J.R., Walters, R.W., Agrawal, A., Barsic, A., and Parker, R. (2016). ATPase-Modulated Stress Granules Contain a Diverse Proteome and Substructure. Cell *164*, 487–498. https://doi.org/10.1016/j.cell.2015.12.038.
17. Kosmacz, M., Gorka, M., Schmidt, S., Luzarowski, M., Moreno, J.C., Szlachetko, J., Leniak, E., Sokolowska, E.M., Sofroni, K., Schnittger, A., and Skirycz, A. (2019). Protein and metabolite composition of Arabidopsis stress granules. New Phytol. *222*, 1420–1433. https://doi.org/10.1111/nph.15690.

18. Buchan, J.R., and Parker, R. (2009). Eukaryotic stress granules: the ins and outs of translation. Mol. Cell *36*, 932–941. https://doi.org/10.1016/j.molcel.2009.11.020.

19. Jang, G.J., Jang, J.C., and Wu, S.H. (2020). Dynamics and Functions of Stress Granules and Processing Bodies in Plants. Plants *9*, 1122. https://doi.org/10.3390/plants9091122.

20. Gutierrez-Beltran, E., Moschou, P.N., Smertenko, A.P., and Bozhkov, P.V. (2015). Tudor staphylococcal nuclease links formation of stress granules and processing bodies with mRNA catabolism in Arabidopsis. Plant Cell *27*, 926–943. https://doi.org/10.1105/tpc.114.134494.

21. Tong, J., Ren, Z., Sun, L., Zhou, S., Yuan, W., Hui, Y., Ci, D., Wang, W., Fan, L.M., Wu, Z., and Qian, W. (2022). ALBA proteins confer thermotolerance through stabilizing HSF messenger RNAs in cytoplasmic granules. Nat. Plants *8*, 778–791. https://doi.org/10.1038/s41477-022-01175-1.

22. Protter, D.S.W., and Parker, R. (2016). Principles and Properties of Stress Granules. Trends Cell Biol. *26*, 668–679. https://doi.org/10.1016/j.tcb.2016.05.004.

23. Sivananthan, S., Gosse, J.T., Huard, S., and Baetz, K. (2023). Pab1 acetylation at K131 decreases stress granule formation in Saccharomyces cerevisiae. J. Biol. Chem. *299*, 102834. https://doi.org/10.1016/j.jbc.2022.102834.

24. Saito, M., Hess, D., Eglinger, J., Fritsch, A.W., Kreysing, M., Weinert, B.T., Choudhary, C., and Matthias, P. (2019). Acetylation of intrinsically disordered regions regulates phase separation. Nat. Chem. Biol. *15*, 51–61. https://doi.org/10.1038/s41589-018-0180-7.

25. Kwon, S., Zhang, Y., and Matthias, P. (2007). The deacetylase HDAC6 is a novel critical component of stress granules involved in the stress response. Genes Dev. *21*, 3381–3394. https://doi.org/10.1101/gad.461107.

26. Maruri-López, I., Figueroa, N.E., Hernández-Sánchez, I.E., and Chodasiewicz, M. (2021). Plant Stress Granules: Trends and Beyond. Front. Plant Sci. *12*, 722643, ARTN. https://doi.org/10.3389/fpls.2021.722643.

27. Kim, S.-C., Guo, L., and Wang, X. (2020). Nuclear moonlighting of cytosolic glyceraldehyde-3-phosphate dehydrogenase regulates Arabidopsis response to heat stress. Nat. Commun. *11*, 3439. https://doi.org/10.1038/s41467-020-17311-4.

28. Lee, H., Guo, Y., Ohta, M., Xiong, L., Stevenson, B., and Zhu, J.K. (2002). LOS2, a genetic locus required for cold-responsive gene transcription encodes a bi-functional enolase. EMBO J. *21*, 2692–2702. https://doi.org/10.1093/emboj/21.11.2692.

29. Liu, X., Wei, W., Zhu, W., Su, L., Xiong, Z., Zhou, M., Zheng, Y., and Zhou, D.X. (2017). Histone Deacetylase AtSRT1 Links Metabolic Flux and Stress Response in Arabidopsis. Mol. Plant *10*, 1510–1522. https://doi.org/10.1016/j.molp.2017.10.010.

30. Mutuku, J.M., and Nose, A. (2012). Changes in the Contents of Metabolites and Enzyme Activities in Rice Plants Responding to Rhizoctonia solani Kuhn Infection: Activation of Glycolysis and Connection to Phenylpropanoid Pathway. Plant Cell Physiol. *53*, 1017–1032. https://doi.org/10.1093/pcp/pcs047.

31. Kosmacz, M., and Skirycz, A. (2020). The Isolation of Stress Granules From Plant Material. Curr. Protoc. Plant Biol. *5*, e20118. https://doi.org/10.1002/cppb.20118.

32. Xu, Q., Wang, Y., Chen, Z., Yue, Y., Huang, H., Wu, B., Liu, Y., Zhou, D.X., and Zhao, Y. (2023). ROS-stimulated protein lysine acetylation is required for crown root development in rice. J. Adv. Res. *48*, 33–46. https://doi.org/10.1016/j.jare.2022.07.010.

33. Xie, Z., Zhao, S., Li, Y., Deng, Y., Shi, Y., Chen, X., Li, Y., Li, H., Chen, C., Wang, X., et al. (2023). Phenolic acid-induced phase separation and translation inhibition mediate plant interspecific competition. Nat. Plants *9*, 1481–1499. https://doi.org/10.1038/s41477-023-01499-6.

34. Wang, Y.P., Zhou, L.S., Zhao, Y.Z., Wang, S.W., Chen, L.L., Liu, L.X., Ling, Z.Q., Hu, F.J., Sun, Y.P., Zhang, J.Y., et al. (2014). Regulation of G6PD acetylation by SIRT2 and KAT9 modulates NADPH homeostasis and cell survival during oxidative stress. EMBO J. *33*, 1304–1320. https://doi.org/10.1002/embj.201387224.

35. Jiang, W., Wang, S., Xiao, M., Lin, Y., Zhou, L., Lei, Q., Xiong, Y., Guan, K.L., and Zhao, S. (2011). Acetylation regulates gluconeogenesis by promoting PEPCK1 degradation via recruiting the UBR5 ubiquitin ligase. Mol. Cell *43*, 33–44. https://doi.org/10.1016/j.molcel.2011.04.028.

36. Du, Z., Song, J., Wang, Y., Zhao, Y., Guda, K., Yang, S., Kao, H.Y., Xu, Y., Willis, J., Markowitz, S.D., et al. (2010). DNMT1 stability is regulated by proteins coordinating deubiquitination and acetylation-driven ubiquitination. Sci. Signal. *3*, ra80. https://doi.org/10.1126/scisignal.2001462.

37. Feid, S.C., Walukiewicz, H.E., Wang, X., Nakayasu, E.S., Rao, C.V., and Wolfe, A.J. (2022). Regulation of Translation by Lysine Acetylation in Escherichia coli. mBio *13*, e0122422. https://doi.org/10.1128/mbio.01224-22.

38. Maruri-Lopez, I., Figueroa, N.E., Hernandez-Sanchez, I.E., and Chodasiewicz, M. (2021). Plant Stress Granules: Trends and Beyond. Front. Plant Sci. *12*, 722643. https://doi.org/10.3389/fpls.2021.722643.

39. Szczerba, M., Johnson, B., Acciai, F., Gogerty, C., McCaughan, M., Williams, J., Kibler, K.V., and Jacobs, B.L. (2023). Canonical cellular stress granules are required for arsenite-induced necroptosis mediated by Z-DNA–binding protein 1. Sci. Signal. *16*, eabq0837. https://doi.org/10.1126/scisignal.abq0837.

40. Herman, A.B., Silva Afonso, M., Kelemen, S.E., Ray, M., Vrakas, C.N., Burke, A.C., Scalia, R.G., Moore, K., and Autieri, M.V. (2019). Regulation of Stress Granule Formation by Inflammation, Vascular Injury, and Atherosclerosis. Arterioscler. Thromb. Vasc. Biol. *39*, 2014–2027. https://doi.org/10.1161/atvbaha.119.313034.

41. Gal, J., Chen, J., Na, D.Y., Tichacek, L., Barnett, K.R., and Zhu, H. (2019). The Acetylation of Lysine-376 of G3BP1 Regulates RNA Binding and Stress Granule Dynamics. Mol. Cell Biol. *39*, e00052-19. https://doi.org/10.1128/MCB.00052-19.

42. Krapp, S., Greiner, E., Amin, B., Sonnewald, U., and Krenz, B. (2017). The stress granule component G3BP is a novel interaction partner for the nuclear shuttle proteins of the nanovirus pea necrotic yellow dwarf virus and geminivirus abutilon mosaic virus. Virus Res. *227*, 6–14. https://doi.org/10.1016/j.virusres.2016.09.021.

43. Yruela, I., Moreno-Yruela, C., and Olsen, C.A. (2021). Zn(2+)-Dependent Histone Deacetylases in Plants: Structure and Evolution. Trends Plant Sci. *26*, 741–757. https://doi.org/10.1016/j.tplants.2020.12.011.

44. Wang, W., Lu, Y., Li, J., Zhang, X., Hu, F., Zhao, Y., and Zhou, D.X. (2021). SnRK1 stimulates the histone H3K27me3 demethylase JMJ705 to regulate a transcriptional switch to control energy homeostasis. Plant Cell *33*, 3721–3742. https://doi.org/10.1093/plcell/koab224.

45. Lei, Y., Lu, L., Liu, H.-Y., Li, S., Xing, F., and Chen, L.-L. (2014). CRISPR-P: A Web Tool for Synthetic Single-Guide RNA Design of CRISPR-System in Plants. Mol. Plant *7*, 1494–1496. https://doi.org/10.1093/mp/ssu044.

46. Gibson, D.G., Young, L., Chuang, R.-Y., Venter, J.C., Hutchison, C.A., and Smith, H.O. (2009). Enzymatic assembly of DNA molecules up to several hundred kilobases. Nat. Methods *6*, 343–345. https://doi.org/10.1038/nmeth.1318.

47. Livak, K.J., and Schmittgen, T.D. (2001). Analysis of relative gene expression data using real-time quantitative PCR and the 2(-Delta Delta C(T)) Method. Methods *25*, 402–408. https://doi.org/10.1006/meth.2001.1262.

48. Emms, D.M., and Kelly, S. (2019). OrthoFinder: phylogenetic orthology inference for comparative genomics. Genome Biol. *20*, 238. https://doi.org/10.1186/s13059-019-1832-y.

49. Szklarczyk, D., Kirsch, R., Koutrouli, M., Nastou, K., Mehryary, F., Hachilif, R., Gable, A.L., Fang, T., Doncheva, N.T., Pyysalo, S., et al. (2023). The STRING database in 2023: protein–protein association networks and functional enrichment analyses for any sequenced genome of interest. Nucleic Acids Res. *51*, D638–D646. https://doi.org/10.1093/nar/gkac1000.

STAR★METHODS

KEY RESOURCES TABLE

REAGENT or RESOURCE	SOURCE	IDENTIFIER
Antibodies		
Mouse Monoclonal Anti-ACTIN	BBI	Cat#D191048
Rabbit polyclonal Anti-HDA714	Xu et al.[11]	https://doi.org/10.1093/nar/gkab244
Rabbit polyclonal Anti-acetyl-lysine	Abcam	Cat#ab21623
Rabbit polyclonal Anti-GAPDH	Abcam	Cat#ab9485
Mouse Monoclonal Anti-ENO1	Abmart	Cat#YM029972M
Mouse Monoclonal Anti-HA	Abclonal	Cat#AE008
Rabbit Monoclonal Anti-RPS6	Abcam	Cat#ab225676
Mouse Monoclonal Anti-MBP	NEB	Cat#E8032S
Rabbit polyclonal Anti-GST	Abcam	Cat#ab9085
Mouse Monoclonal Anti-FLAG	Sigma-Aldrich	Cat#F3165
Bacterial and virus strains		
Escherichia coli strain DH5α	Tsingke	Cat#TSC-C01
Escherichia coli BL21	Tsingke	Cat#TSC-E01
Agrobacterium tumefaciens strain EHA105	Tsingke	Cat#TSC-A03
Chemicals, peptides, and recombinant proteins		
Protease Inhibitor Cocktail, EDTA free	Roche	Cat# 04693132001
4% PFA fixative	Biosharp	Cat#BL539A
HiScript II Q RT SuperMix for qPCR	Vazyme	Cat#R222-01
Cycloheximide	Sigma-Aldrich	Cat#C7698
Trichostatin A	Selleckchem	Cat#S1045
SuperKine™ Enhanced Antifade Mounting Medium with DAPI	Abbkine	Cat#BMU107
Macerozyme R-10	Yakult	Cat#L0021
Cellulase R-10	Yakult	Cat#L0012
Critical commercial assays		
Taq Pro Universal SYBR qPCR Master Mix	Vazyme	Cat# Q712-02
D-Luciferin, Sodium Salt	Yeasen	Cat# 40901ES03
Glyceraldehyde-3-phosphatedehydrogenase Assay Kit	Comin	Cat#GAPDH-1-Y
Pyruvate Kinase Assay Kit	Comin	Cat#PK-1-Y
Enolase Activity Assay Kit	Sigma-Aldrich	Cat#MAK178
Deposited data		
The SG mass spectrometry data	ProteomeXchage	PXD043593
The *hda714* acetylome data	ProteomeXchage	PXD014063
The heat stress acetylome data	ProteomeXchage	PXD053060
Experimental models: Organisms/strains		
Oryza Sativa: Zhonghua 11	Xu et al.[11]	N/A
Oryza Sativa: hda714#1	Xu et al.[11]	N/A
Oryza Sativa: hda714#2	This paper	N/A
Oryza Sativa: HDA714OE#1	Xu et al.[11]	N/A
Oryza Sativa: HDA714OE#2	Xu et al.[11]	N/A
Oryza Sativa: hda705#1	Xu et al.[11]	N/A
Oryza Sativa: hda705#2	Xu et al.[11]	N/A
Oryza Sativa: hda706#1	Xu et al.[11]	N/A
Oryza Sativa: hda706#2	Xu et al.[11]	N/A
Oryza Sativa: OE-PK3	This paper	N/A

(*Continued on next page*)

Continued

REAGENT or RESOURCE	SOURCE	IDENTIFIER
Oryza Sativa: OE-TSN	This paper	N/A
Oryza Sativa: Com#1	This paper	N/A
Oryza Sativa: Com#2	This paper	N/A
Nicotiana benthamiana	This paper	N/A
Oligonucleotides		
Primers for vectors construction, see Data S6	This paper	N/A
Recombinant DNA		
35S:HDA714-GFP	This paper	N/A
35S:RBP47B-RFP	This paper	N/A
35S:TSN2-RFP	This paper	N/A
35S:HDA706-GFP	This paper	N/A
35S:HDA706-RFP	This paper	N/A
ENO1-GST	This paper	N/A
GAPDH1-GST	This paper	N/A
TSN-GST	This paper	N/A
HDA714-MBP	This paper	N/A
35S:PABP1-GFP	This paper	N/A
35S:PABP3-GFP	This paper	N/A
35S: TSN-GFP	This paper	N/A
35S:DEAD-GFP	This paper	N/A
35S:PK3-GFP	This paper	N/A
35S:RPS6-GFP	This paper	N/A
35S:RPS3-GFP	This paper	N/A
35S: EIF-GFP	This paper	N/A
35S: HDA714-cYFP	This paper	N/A
35S: TSN-nYFP	This paper	N/A
35S:PK3-nYFP	This paper	N/A
35S:WOX11-nYFP	This paper	N/A
35S:HDA714-nLUC	This paper	N/A
35S:TSN-cLUC	This paper	N/A
35S:PK3-cLUC	This paper	N/A
35S:WOX11-cLUC	This paper	N/A
Ubi:TSN-FLAG	This paper	N/A
Ubi:PK3-FLAG	This paper	N/A
Software and algorithms		
ImageJ	NIH	https://imagej.nih.gov/ij/
GraphPad Prism 9	GraphPad Prism	https://www.graphpad-prism.cn/

RESOURCE AVAILABILITY

Lead contact

Further information and requests for resources and reagents should be directed to and will be fulfilled by the lead contact, Dao-Xiu Zhou (dao-xiu.zhou@universite-paris-saclay.fr).

Materials availability

The plants and plasmids generated in this work can be requested from the lead contact. This study did not generate new unique reagents.

Data and code availability

- The SG mass and acetylome spectrometry data have been deposited online at the ProteomeXchage and is publicly accessible as of the publication date. The dataset identifier is listed in the key resources table.

- This paper does not report original code.
- Any additional information required to reanalyze the data reported in this work is available from the lead contact upon request.

EXPERIMENTAL MODEL AND STUDY PARTICIPANT DETAILS

Rice and N. benthamiana

In this study, the rice variety Zhonghua11 *(Oryza sativa* spp. *Japonica*) was used to produce the transgenic plants. The CRISPR/Cas9[41] mutants were produced by transformation of the binary transfer DNA vectors containing Cas9 and sgRNA into rice calli. The mutation was decoded by DSDecode.[42] The over expression transgenic plants were produced using the maize (*Zea mays*) ubiquitin promoter vector pU1301-3×FLAG.

METHOD DETAILS

Plant materials and stress treatments

For the *hda714* mutants, two independent transgenic lines (Cas9 free) were used, which included the previously reported CRISPR/Cas9-generated *hda714* mutant line (*hda714#1*) was utilized in this study,[11] and *hda714#2* which was generated in this study with a different sgRNA targeting the *HDA714* gene (Figure S1A, see below). The *had705* and *hda706* mutants used in this study were characterized in a previous study.[11] The *HDA714, TSN*, and *PK3* overexpression lines were generated by fusing the FLAG tag to the C terminus of the coding sequences, driven by the ubiquitin promoter. Two independent *HDA714, TSN* or *PK3* over-expression lines were obtained. The *pk1* complementation lines (*Com#1* and *Com#2*) were driven by their own promoters, with the CDS HA-tagged. Transgenic plants were produced using the rice variety Zhonghua11 (*Oryza sativa* ssp. *Japonica* [Geng]). For phenotyping, plants were hydroponically cultivated in liquid Yoshida's solution.[44] Various stress treatments were applied to seedlings at the early developmental stage. For cold stress, 14-day-old seedlings grown hydroponically of 25°C/14 h light and 25°C/10 h dark were transferred to a 4°C chamber for 3 days. For heat stress, seedlings were incubated at 42°C in a growth chamber for 5–7 days. For salt and osmotic stresses, NaCl (180 mM) and PEG6000 (20%) were added to the nutrient solution for 3 and 4 days, respectively. For the control, seedlings were grown under normal conditions of 25°C/14 h light and 25°C/10 h dark. After stress treatments, seedlings were returned to normal conditions for 7 days before surveying survival rates based on the percentage of viable seedlings. The survival rates (live plants/total plants × 100%) after recovery were surveyed in 3 biological replicates (n = 40 for each replicate). To identify rice thermotolerance at the reproductive stage, rice plants were first grown individually in pots (n > 18) under normal growth conditions (30°C/13 h light, 25°C/11 h dark) in a greenhouse. At the flowering stage, half of the plants were then subjected to high-temperature stress (37°C/13 h light, 25°C/11 h dark) for 14 days, while the other half was kept under standard growth conditions. After the treatment, the plants were returned to standard growth conditions until maturation, and the phenotypes were assayed.

CRISPR/Cas9 vector construction

The CRISPR/Cas9 sgRNAs targeting *HDA714* gene were designed using CRISPR-P2.0 (http://crispr.hzau.edu.cn/CRISPR2/). The transgenic vectors were constructed as previously described.[45] The Cas9 and sgRNA expression cassettes were driven by the ubiquitin promoter and U3/6 promoter, respectively. The sgRNAs were then ligated into the Cas9 destination vector using Gibson Assembly Cloning.[46] The resulting transfer DNA vectors, containing both Cas9 and the sgRNAs, were transformed into rice calli via *Agrobacterium*-mediated transformation.

RT-qPCR

Total RNA was extracted using TRIzol reagent (Invitrogen, 15596018). Complementary DNA was synthesized from 1 μg of RNA using the reverse transcription kit (Vazyme, R212-01). Real-time PCR was performed using the SYBR Premix ExTaq (Vazyme, Q441-02) on an ABI 7500 real-time PCR instrument, with rice *ACTIN1* serving as the internal standard for gene expression. Each sample was analyzed in triplicate. The relative expression levels were calculated using the $2^{-\triangle\triangle CT}$ method.[47]

Total protein extraction and immunoblotting

To extract total protein, the rice seedlings grown under heat stress and normal conditions were first collected and ground into a fine powder using liquid nitrogen and then homogenized in lysis buffer containing 10 mM Tris-HCl pH7.5, 150 mM NaCl, 0.5 mM EDTA, and 0.5% NP-40. The suspension was then centrifuged at 16,000 g for 10 min at 4°C, and the resulting supernatant was transferred to a new 1.5 mL centrifuge tube. Half of the volume of 2x SDS loading buffer (containing 120 mM Tris-HCl pH 6.8, 20% glycerol, 4% SDS, 0.04% bromophenol blue, and 10% β-mercaptoethanol) was added to the supernatant, and the mixture was thoroughly mixed before being heated at 95°C for 10 min. The extracted total proteins were then used for immunoblotting analysis, using anti-ACTIN (1:4000, D191048-0100, Sangon), anti-Lys-Ac (1:1000, ab21623, Abcam) antibodies, anti-GAPDH (1:1000, ab9485, Abcam), anti-ENO1 (1:1000, YM029972M, Abmart), and anti-HDA714 (1:1000, self-made). Band intensities were quantified from the 16-bit digital image by densitometry in ImageJ (v1.6.0_24) and normalized to the control samples as indicated in the figures.

In vitro deacetylation assays

In vitro deacetylation assays for ENO1, TSN, and GAPDH1 were performed using MBP-tagged HDA714 and GST-tagged ENO1, TSN, and GAPDH1 proteins, which were expressed and purified from *E. coli* cells. The tagged proteins were acetylated in *E. coli*. Deacetylation experiments were conducted at 37°C for 12 h in a reaction buffer containing 50 mM Tris (pH 8.0), 137 mM NaCl, 2.7 mM KCl, 1 mM $MgCl_2$, 1 μM $ZnCl_2$, and 1 mM DTT. The products were then subjected to western blot analysis using an anti-LysAc antibody (1:1000, ab21623, Abcam).

Rice stress granule isolation and proteome identification

Stress granules were also extracted as previously described.[31] In brief, the plant sample (4 g) was finely ground with liquid nitrogen and suspended in lysis buffer (50 mM Tris-HCl pH 7.4, 100 mM potassium acetate, 2 mM magnesium acetate, 0.5% NP-40, 0.5 mM DTT, 1 mM NaF, 1 mM Na_3VO_4, protease inhibitor cocktail, and 1U RNasin). The slurry was centrifuged at 4,000 g for 10 min at 4°C, and the supernatant was removed. The pellet was resuspended in lysis buffer, centrifuged at 18,000 g for 10 min at 4°C, and this process was repeated once, resuspending the pellet in lysis buffer each time. The suspension was then centrifuged at 1000 g for 10 min at 4°C. The resulting supernatant was considered the SG-enriched fraction. A volume of 260 μL of protein-A magnetic beads (Thermo Fisher Scientific, 10001D) was washed once with DEPC-treated PBS buffer supplemented with 0.05% NP-40, followed by three washes with lysis buffer for 5 min at 4°C. The SG-enriched fraction and RNasin (at a final dilution of 1:100) were added to the mixture and incubated on a tube rotator for 15 min at room temperature. The beads were separated using a magnet, and the supernatant was then incubated with anti-HDA714 antibody for 4 h at 4°C. Excess antibody was removed by centrifugation, and the pellet was resuspended in 500 μL of lysis buffer and incubated overnight with 100 μL of equilibrated Dynabeads at 4°C. The protein-bound beads were washed four times with lysis buffer and subsequently sent to BGI Genomics Co., Ltd (China) for mass spectrometric analysis. This process was independently replicated three times for biological validation.

SG proteomics and data analysis

SGs proteins were first trypsin-digested for 4 h at 37°C, followed by desalting and freeze-drying. The resulting dried peptide samples were subsequently reconstituted using mobile phase A (2% ACN, 0.1% FA). The separation process was carried out using a Thermo UltiMate 3000 UHPLC system. The sample was initially enriched in a trap column, underwent desalting, and then entered a self-packed C18 column (75 μm internal diameter, 3μm column size, 25cm column length). Separation occurred at a flow rate of 300 nL/min, following this gradient: 0–5 min, 5% mobile phase B (98% ACN, 0.1% FA); 5–45 min, linear increase of mobile phase B from 5% to 25%; 45–50 min, mobile phase B increased from 25% to 35%; 50–52 min, mobile phase B rose from 35% to 80%; 52–54 min, 80% mobile phase B; 54–60 min, 5% mobile phase B. The nanoliter liquid phase separation end was directly linked to the mass spectrometer. Subsequently, the peptides separated through liquid phase chromatography were ionized using a nanoESI source and then directed to the tandem mass spectrometer Q-Exactive HF (Thermo Fisher Scientific, San Jose, CA) for protein identification. Proteins were identified through a database search of the fragment spectra against the MSU *Oryza sativa* database (http://rice.uga.edu/), concatenated with a reverse decoy database, using the Mascot software program (version 2.3; Matrix Science). An e-value of <0.05 was set as the filtering criterion. Proteins with >2 unique peptides in three biological replicates in either the control or treatment group were selected. By eliminating the proteins present in the control group and proteins annotated as 'mitochondrial' or 'chloroplastic' by cropPAL2, a list of proteins specific to the treatment group were obtained. The protein orthologs between rice, Arabidopsis and human SG proteins were searched using the ortholog tool OrthoFinder (v2.5.4)[48] with default parameters for pairwise searches. GO enrichment was analyzed by PANTHER, domain enrichment analysis was done by STRING (v12.0),[49] and the acetylation status of rice SG proteins was determined based on previously reported protein acetylomes of rice seedlings grown under normal conditions.[11]

Analysis of rice SG proteins acetylation levels

SG fractions from wild type, *hda714* mutants, and *HDA714* overexpression plants rice seedlings under heat stress were isolated as described above. The lysine acetylation levels of SG fraction proteins were assayed by immunoblotting using an anti-LysAc antibody, which detects only acetylated proteins.

To analyze RPS6 acetylation, the isolated SG fractions from the different genotypes were dissolved in buffer X (50 mM HEPES-KOH [pH 7.5], 150 mM NaCl, 1 mM Ethylene Diamine Tetraacetic Acid [EDTA], 1% Triton X-100, 0.1% sodium deoxycholate, 0.1% SDS). Subsequently, the dissolved proteins were incubated with anti-RPS6 (1:1000, ab40820, Abcam) coated protein-A magnetic beads (Thermo Fisher Scientific, 10001D) for 5 h at 4°C. After four washes with PBST buffer, the immuno-purified proteins were collected. After boiled at 95°C, the purified proteins were separated by SDS-PAGE and immunoblotted with anti-RPS6 (1:1000, ab127980, Abcam) and anti-LysAc (1:1000, ab21623, Abcam).

Bimolecular fluorescence complementation (BiFC) assay

For the BiFC assays, *Agrobacterium* strains EHA105 carrying cYFP-HDA714 and the nYFP-TSN or nYFP-PK3 were co-infiltrated into *N. benthamiana* leaves. After 48 h, the plants (n = 3) were treated at 42°C for 30 min, with the control plants maintained at normal temperature (25°C). The transfected leaf cells were then photographed using a laser confocal microscope (Olympus FV1200).

Split-luciferase complementation assays

For the split-luciferase complementation assays, the constructs containing split luciferase (nLUC- and cLUC) were initially introduced into *A. tumefaciens* cells. Subsequently, the designated pairs of transformed constructs were infiltrated into the abaxial epidermis of 6-week-old tobacco (*N. benthamiana*) leaves using a needleless syringe. At least three tobacco plants ($n = 3$) were infiltrated. After 48 h of transfection, the transfected leaves were treated with 1 mM luciferin (Gold Biotechnology) and kept in darkness for 10 min. Luciferase bioluminescence images were captured using the Chemi-Image System (Tanon 5200Multi).

In vitro pull-down assays

For *in vitro* pull-down assays, GST-tagged PK3, GST-tagged HDA714, MBP-tagged TSN and MBP-tagged HDA714 were constructed and expressed in the *Escherichia coli* cells. GST or PK3-GST coupled GST beads (17-5132-01, GE Healthcare) were used to pull down HDA714-MBP and analyzed by immunoblotting with anti-MBP antibody (1:4000, E8032S, NEB). TSN-MBP was incubated with GST or HDA714-GST and pulled down with GST beads. Anti-MBP antibody was used to detect TSN-MBP by immunoblotting.

Co-IP assays

For co-immunoprecipitation to detect *in vivo* interaction between HDA714 and TSN or PK3 proteins, *TSN-FLAG* and *PK3-FLAG* overexpression seedlings were pulverized into powder using liquid nitrogen and then extracted with lysis buffer (10 mM Tris–HCl pH 7.5, 150 mM NaCl, 0.5 mM EDTA, 0.5% Nonidet P40 Substitute). The extracts were incubated with anti-FLAG M2 magnetic beads (M8823, Sigma) for 5 h at 4°C. After four washes with PBST buffer, the co-immunoprecipitated proteins were separated by SDS-PAGE and analyzed by immunoblotting using anti-FLAG (1:1000, F3165, Sigma) and anti-HDA714 (1:1,000, self-made) antibodies.

LC-MS/MS-based quantitative acetylproteomics

The control and heat-stressed rice seedlings (exposed to 42°C for 72 h) were collected, ground to powder using liquid nitrogen, and then phenol extraction buffer (containing 10 mM dithiothreitol, 1% protease inhibitor, 3 μM TSA, 50 mM NAM) was added for ultrasonic lysis. After centrifugation, the supernatant was mixed with an equal volume of Tris-balanced phenol to precipitate overnight. The resulting precipitates were washed five times with 0.1 M ammonium acetate/methanol. The precipitates were then dissolved in 8 M urea. For acetylproteomics, the protein solution was first treated with 5 mM dithiothreitol at 56°C for 30 min, then with 11 mM iodoacetamide at 25°C for 15 min in the dark. The urea concentration was reduced to less than 2 M with 100 mM TEAB. Then, trypsin was added at a 1:50 ratio for 12 h and at a 1:100 ratio for 4 h. Peptides were next dissolved in IP buffer (100 mM NaCl, 50 mM Tris-HCl, 1 mM EDTA, 0.5% NP-40, pH 8.0) with antibody beads (PTM-104, PTM Bio) and mixed at 4°C for 12 h. After washing, peptides were eluted with 0.1% trifluoroacetic acid, collected, and dried. For LC-MS/MS analysis, peptides were first desalted using C18 ZipTips (Millipore) and then separated using a NanoElute system with mobile phases of 0.1% formic acid (A) and 0.1% formic acid in acetonitrile (B). The gradient was: 0–40 min, 7%–24% B; 40–52 min, 24%–32% B; 52–56 min, 32%–80% B; 56–60 min, 80% B, at 450 nL/min. The final peptides were ionized and analyzed with a TIMS-TOF Pro mass spectrometer. The scan range was 100–1700 m/z in PASEF mode. The resulting MS/MS data were analyzed using MaxQuant (v1.6.15.0) with the *Oryza_sativa*_4530_NCBI database. Trypsin/P was set for digestion with up to 4 missed cleavages. Modifications included fixed cysteine alkylation and variable methionine oxidation, N-terminal acetylation, lysine acetylation, and deamidation. Identifications with FDR <1% were selected. Proteins that exhibited less than 1-fold change in Kac levels in both replicates were annotated as decreased.

Stress granule assays in *Nicotiana benthamiana* cells

The full-length cDNAs of the target genes of *RPS6* (Os07g0622100), *TSN* (Os02g0523500), *PABP1* (Os09g0115400), *RPS3* (Os03g0577000), *PK1* (Os11g0148500), *PK3* (Os04g0677500), *DEAD* (Os04g0533000), *PABP3* (Os04g0504800), *EIF* (Os02g0519900), *RBP47B* (AT3G19130), and *TSN* (AT5G61780) were subcloned into pCambia 1301. RBP47B and TSN were specifically fused with RFP, whereas the remaining genes were fused with GFP. *A. tumefaciens* cells with above constructs were infiltrated into the abaxial epidermis of 6-week-old tobacco (*N. benthamiana*) leaves using a syringe. After 48 h, the plants were subjected to 42°C for 30 min, while the control plants were maintained under normal growth conditions. The leaf cells were then photographed using a laser confocal microscope (Olympus FV1200). For each transient expression experiment, at least three ($n = 3$) tobacco plants were infiltrated. After 48 h, the plants were treated at 42°C for 30 min, the leaf cells were photographed using a laser confocal microscope (Olympus FV1200). The image was quantified using ImageJ (v1.41) software, and the number of SG was quantified in every 1000 μm^2. For co-localization analyses, we calculated the Pearson correlation coefficient (PCC) for the pixels representing the fluorescence signals in both channels. A sample size of $n = 6$ was used for Pearson correlation coefficient (PCC) quantification, and the results are presented as mean ± SD. Levels of co-localization range from +1 to −1 for positive and negative correlations, respectively.

Immunofluorescence staining of rice root tips

The root tips of 3-day-old rice seedlings were either treated at 42°C for 6 h or untreated as a control. For the Cycloheximide (CHX) treatment, the seedling roots were first pre-incubated with 200 ng/L CHX for 30 min and then heat-stressed at 42°C for 6 h. For the Trichostatin A (TSA) treatment, the seedling roots were incubated with 3 μM TSA for 30 min and then heat-stressed at 42°C for 6 h. The root tips were fixed with 4% paraformaldehyde for 30 min at room temperature and then digested with 3% (w/v) cellulase R-10

and 0.3% (w/v) Macerozyme R-10 (Yakult Pharmaceutical Industry) for 4 h at 37°C. Then the root tips were placed on a polyline-coated slide, which was prepared using the squashed method.

For immunofluorescence staining, the prepared slides were blocked with 5% (w/v) bovine serum albumin in PBS (pH7.4) for 1 h at 37°C, and then washed three times with PBS. Next, the slides were incubated with primary antibodies diluted 1:100 at 4°C overnight, followed by secondary antibodies diluted 1:200 at 37°C for 1 h after three washes with PBS. Each slide was then stained with DAPI and photographed using a microscope (Olympus FV1200) in Airyscan mode with a ×60 NA oil objective. The SG numbers in immunostained rice root tip cells were individually quantified with ImageJ (v1.41).

Enzyme activity assays

The activities of the glycolytic enzymes GAPDH and PK were determined using commercial kits (Suzhou Keming Biotechnology) following the manufacturer's instructions. In brief, 0.1 g of rice seedlings was homogenized in 1 mL of enzyme extraction buffer and then centrifuged at 4°C for 10 min. The absorbance was measured at a wavelength of 340 nm using a multimode microplate reader (Spark, TECAN). Six biological replicates were performed for each genotype. Enzyme activity was calculated from the absorbance value and the sample fresh weight using the formula provided in the enzyme kit instructions.

Enolase activity was determined using the Enolase Activity Assay Kit (Sigma, Germany, MAK178-1KT) according to the manufacturer's instructions. In brief, 0.01 g of rice seedlings was homogenized in 100 μL of ice-cold Enolase Assay Buffer and then centrifuged at 4°C for 5 min. The samples of cell lysates were mixed with reaction buffer and incubated at 25°C. After 5–10 min, an initial measurement of the OD value was taken at a wavelength of 570 nm. This was followed by measurements every 2–3 min until the OD value reached its highest point. The enzyme activity of the sample was calculated according to the instructions provided in the kit.

Stress granule assays in rice protoplasts

The full-length cDNAs of the target genes were subcloned into pCambia1301 to fuse with GFP. The fusion was transiently expressed in rice protoplasts using polyethylene glycol-mediated transformation. After overnight culture, the subcellular localization was visualized using a confocal laser scanning microscope (Olympus FV1200) under normal (25°C) and heat stress (42°C for 30 min).

QUANTIFICATION AND STATISTICAL ANALYSIS

All the data were analyzed using one-way ANOVA or Student's t test. The values represented as means ± standard deviation (SD). Statistical details can be found in the figure legends, including biological repeats, exact value of n, what n represents, and the statistical tests used.